Miner Deposita (2014) 49:489–512
DOI 10.1007/s00126-013-0499-7

ARTICLE

The Key Tuffite, Matagami Camp, Abitibi Greenstone Belt, Canada: petrogenesis and implications for VMS formation and exploration

Dominique Genna · Damien Gaboury · Gilles Roy

Received: 21 February 2013 / Accepted: 20 November 2013 / Published online: 29 December 2013

Abstract The Key Tuffite is a stratigraphic marker unit for most of the zinc-rich volcanogenic massive sulfide deposits of the Matagami Camp in the Abitibi Greenstone Belt. This 2- to 6-m-thick unit was previously interpreted as a mixture of ash fall (andesitic to rhyolitic tuffaceous components) and volcanogenic massive sulfide (VMS)-related chemical seafloor precipitate (exhalative component). Previous attempts to develop geochemical exploration vectoring tools using metal content within the Key Tuffite were mostly inconclusive due to the complex nature of the Key Tuffite unit and a poor understanding of its composition, origin and relationship with the VMS-forming hydrothermal systems. Detailed mapping and thorough lithogeochemistry of the Key Tuffite in the vicinity of the Perseverance and Bracemac-McLeod deposits indicate that the Key Tuffite is a homogeneous calc-alkaline, andesitic tuff that was deposited before the VMS deposits were formed. The unit is mostly devoid of exhalative component, but it is strongly hydrothermally altered close to orebodies. This is characterized by a strong proximal chloritization and a distal sericitization, which grades laterally into the unaltered Key Tuffite. Neither the Key Tuffite nor the ore was formed by seafloor exhalative processes for the two studied deposits. This probably explains why previously proposed exploration models based on metal scavenging proved unsuccessful and suggests that a re-evaluation of the exhalative model should be done at the scale of the mining camp. However, as shown in this study, hydrothermal alteration can be used to vector towards ore along the Key Tuffite.

Keywords VMS · Exhalite · Replacement · Abitibi · Matagami · Bracemac-McLeod · Perseverance

Editorial handling: G. Beaudoin

Electronic supplementary material The online version of this article (doi:10.1007/s00126-013-0499-7) contains supplementary material, which is available to authorized users.

D. Genna (✉) · D. Gaboury
Experimental and Quantitative Metallogeny Research Laboratory (LAMEQ), Université du Québec à Chicoutimi, 555 boul. de l'Université, Chicoutimi, Quebec G7H 2B1, Canada
e-mail: gennadomi@hotmail.com

G. Roy
Glencore, Bureau d'exploration Matagami, C.P. 819, Matagami, Quebec J0Y 2A0, Canada

Introduction

Since the discovery of the Matagami mining camp (Quebec, Canada) in the Archean Abitibi Greenstone Belt at the end of the 1950s, there has been a debate over the origin of the zinc-rich volcanogenic massive sulfide (VMS) deposits. Two schools of thought exist. Originally, most of the early workers regarded the ore deposits as epigenetic bodies formed by replacement processes (Miller 1960; Jenney 1961; Hallam 1964; Tully 1964; Sharpe 1968). Latulippe (1959) was however the first to propose that most of the features were compatible with a syngenetic exhalative origin, with the main argument based on the association of all the mined deposits with a regional stratigraphic marker known as the Key Tuffite (Miller 1960). The Key Tuffite is a laterally extensive (~17 km), continuous and thinly layered tuffaceous to cherty unit that is 2 to 6 m thick on average (Fig. 1). This unit has been used as a first-order vector for exploration in the camp for the last 50 years. The discovery of sulfide chimney and mound deposits on the modern seafloor (e.g. Corliss et al. 1979) at the end of the 1970s gave credence to the exhalative model. Since then, this model has been generally accepted for the Matagami mining camp (Roberts 1975; Roberts and Reardon 1978; MacGeehan and MacLean 1980; Costa et al. 1983; Ioannou et al. 2007). As such, Matagami is often quoted as a classical example of exhalative-style mineralization.

However, the atypical geometry of the last two VMS discoveries at Matagami, the Perseverance (Arnold 2006) and Bracemac-McLeod (Adair 2009) deposits, challenges the accepted ore-forming exhalative model. The Perseverance mine consists of three sub-vertical orebodies overlain by a sub-horizontal, barren, but strongly silicified, Key Tuffite. In contrast, the Bracemac-McLeod mine consists of (1) two main sheet-like massive sulfide deposits (Bracemac and McLeod) occurring at the Key Tuffite stratigraphic interval which exhibit both stratabound and crosscutting relationships and, (2) in the Bracemac deposit, two sheet-like massive sulfide lenses located 180 and 270 m stratigraphically above the Key Tuffite, respectively.

In this contribution, the geological setting of the Perseverance and Bracemac-McLeod deposits is described with an emphasis on the nature and origin of the Key Tuffite and its relationship with the ore-forming hydrothermal systems. Previous studies concluded that the Key Tuffite was the result of the mixing of at least two components in varying proportions: (1) tuffaceous (ash) and (2) exhalative (Davidson 1977). However, proposed geochemical vectoring tools based on these considerations were mostly inconclusive at Matagami (MacLean and Davidson 1977), contrary to other VMS districts where exploration vectors based on exhalative units proved to be successful, such as in the Bathurst camp, Canada (Peter and Goodfellow 2003) and the Hokuroku District, Japan (Kalogeropoulos and Scott 1983). Moreover, most ancient VMS deposits have undergone post-ore, late-stage episodes of hydrothermal alteration and/or seafloor and regional metamorphism, which can alter primary features of tuffaceous exhalites (Franklin et al. 1981; Large 1992). Therefore, a third component must be taken into consideration when characterizing tuffaceous exhalites and trying to develop geochemical exploration vectors: epigenetic hydrothermal alteration. Although the term epigenetic generally refers to much later events, it is used here to describe all the hydrothermal processes that might have modified the composition of the Key Tuffite after its deposition, which comprises the alteration and mineralization still synvolcanic in origin.

The three components of the Key Tuffite (tuffaceous, exhalative and hydrothermal) were independently characterized using field observations, geometric relationships and geochemical data. Our study indicates that the Key Tuffite, although representing a major break in effusive volcanic activity, is not an exhalite unit sensu stricto. The Key Tuffite is now interpreted as a homogeneous calc-alkaline andesitic tuff mostly devoid of exhalative component that is however strongly hydrothermally altered proximal to VMS hydrothermal systems. These features, combined with geometric relationships between the Key Tuffite and the orebody shapes, imply that the mineralization was mostly formed by subseafloor replacement, in agreement with mine-scale observations. Neither the tuffite nor the mineralization was dominantly formed by seafloor exhalative processes, explaining why exploration tools proposed in the past based on metal scavenging were not efficient. However, our study of the Perseverance and Bracemac-McLeod deposits indicates that hydrothermal alteration along the Key Tuffite has a real potential to be used as an exploration tool.

Regional geology

The Archean Abitibi Greenstone Belt in Canada is the largest (300×700 km) and also one of the richest greenstone belts in the world with approximately 90 VMS deposits (Card 1990; Allen and Weihed 2002; Mercier-Langevin et al. 2011). The Abitibi Greenstone Belt is an east-trending volcano-sedimentary sequence intruded by plutonic suites that display evidence of arc evolution, arc–arc collision and arc fragmentation dating from 2,735 to 2,670 Ma (Daigneault et al. 2004; Mueller et al. 1996, 2009).

The 2.7-Ga (Mortensen 1993; Ross et al. 2014) Matagami mining camp (Fig. 1) is located in the northern part of the Abitibi belt close to the boundary with the Opatica sub-province to the north. The camp constitutes an important zinc district with more than 60 Mt of zinc-rich ore (19 deposits and prospects, including 13 past and current producers; Mercier-Langevin et al. 2014; Ross et al. 2014). All of the known VMS deposits of the camp are spatially associated with extensive felsic bands that are divided into the north flank, the south flank and the west camp (Fig. 1). The intensity of deformation is higher on the north flank compared to the other felsic bands (Piché et al. 1993) because of its proximity to the Opatica sub-province boundary (Pilote et al. 2011). Regional metamorphism generally reached greenschist facies but locally amphibolite facies on the north flank (Jolly 1978). Despite numerous studies (e.g. Jenney 1961; Sharpe 1968; Roberts 1975; Beaudry and Gaucher 1986; Piché et al. 1990), the understanding of the camp remains limited in part because of the scarcity of outcrops.

The general volcanic stratigraphy of the camp, as proposed by Sharpe (1968) and validated by Piché et al. (1990), is divided into the Watson Lake Group at the base and the Wabassee Group at the top (Fig. 1b). The Key Tuffite and all the major deposits are located at the interface of these groups. The Watson Lake Group is composed of two felsic units: (1) a poorly exposed lower dacite (500 m thick minimum; Piché et al. 1993) and (2) an upper rhyolite (1,500 m thick), termed the Watson rhyolite (2,725.9±0.8 Ma; Ross et al. 2014). Both show good evidence of submarine volcanic textures (Piché et al. 1993; Debreil and Ross 2009). According to the

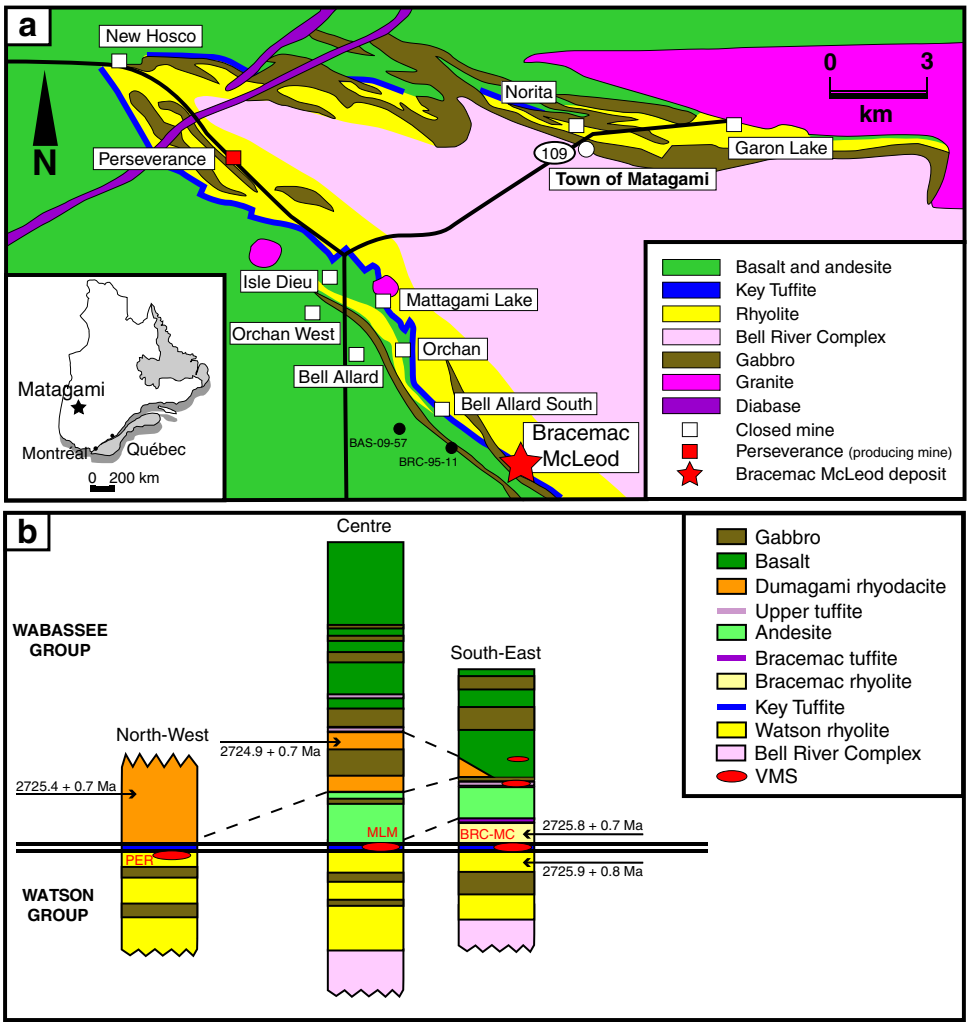

Fig. 1 Geological setting of the Matagami mining camp. **a** Simplified regional map (modified from Glencore). The west camp is not presented here. **b** Stratigraphic columns along the south flank. Ages from Ross et al. (2014). *PER* Perseverance, *MLM* Mattagami Lake Mine, *BRC-MC* Bracemac-McLeod

geochemical classification of rhyolites associated with VMS mineralization (Lesher et al. 1986; Hart et al. 2004), the Watson rhyolite (FIIIb type) is considered particularly fertile (Gaboury and Pearson 2008). The Wabassee Group (3,000 m thick) mostly comprises massive or pillowed mafic lavas of basaltic and andesitic composition. However, two felsic units are present in the Wabassee Group along the south flank (Fig. 1b). At the Perseverance mine, the hanging wall is the Dumagami rhyolite (up to 400 m thick), whereas the Bracemac rhyolite (up to 70 m thick) is the hanging wall of the Bracemac-McLeod deposits. The ages of these two rhyolites are 2,725.4±0.7 and 2,725.8±0.7 Ma, respectively (Ross et al. 2014). Both the Watson Lake and the Wabassee Groups are locally crosscut by late phases of the underlying Bell River Complex, a large synvolcanic tholeiitic gabbro-anorthosite-layered intrusion dated at 2,724.6±2.5 Ma (Mortensen 1993). This intrusion is interpreted as the source for the overlying volcanic units and as the thermal source for the formation of the VMS deposits (Piché et al. 1990; Maier et al. 1996; Ioannou and Spooner 2007; Carr et al. 2008).

The Key Tuffite

The Key Tuffite lies at the interface between the Watson and the Wabassee Groups. It is a continuous unit which is 0.1 to 10 m thick and extends for over ~17 km on strike in a north-west–south-east direction. Recent work on the west camp suggests that the Key Tuffite could also be present west of the south flank (Masson 2000; Bussières and Théberge 2006), increasing significantly the lateral extension of the Key Tuffite (>20 km). Observations by many authors on the Key Tuffite in the vicinity of VMS deposits along the south flank lead to the following characteristics, which over time have been assumed to be representative of the Key Tuffite at the camp scale:

– The Key Tuffite is mostly delicately layered (e.g. Davidson 1977; Costa et al. 1983; Liaghat and MacLean 1992) and divided in three major zones: an upper fragmental zone, a central well-bedded cherty zone and a lower tuff zone with some larger fragments resembling the Watson rhyolite. One or even two of these zones can be missing in some sections (Davidson 1977).
– The Key Tuffite is composed of volcanic ash altered to chlorite and sericite and mixed with chemical sediments, including chert, sulfides and carbonates (Davidson 1977; Liaghat and MacLean 1992).

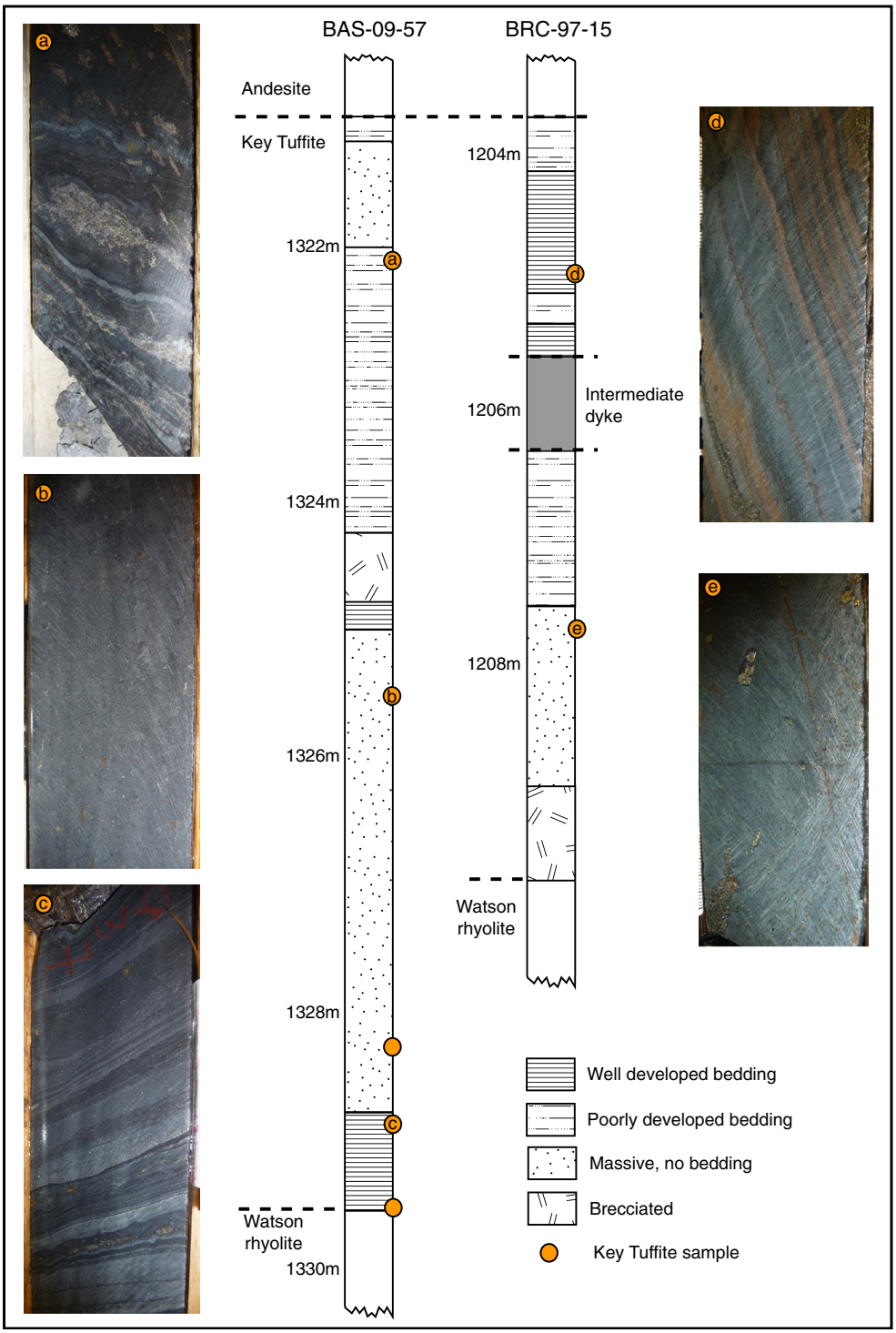

Fig. 2 Detailed section of the Key Tuffite in two drill holes (BAS-09-57 and BRC-97-15) away from any known mineralization (>1 km). The location of the drill holes, projected to the surface, is shown in Fig. 1

– The average metallic content is high (1.4 % Zn, 0.1 % Cu and anomalous values of Pb, Co, Ni and Cr) as reported in the vicinity of the Bell Allard South deposit by Davidson (1977).

However, these observations on the Key Tuffite are not necessarily valid away from mineralization and alteration. Figure 2 presents two sections of Key Tuffite both located at >1 km away from any known deposit. Their position in the mining camp is illustrated in Fig. 1. Four main textural features are identified regarding layering: well or poorly developed layering, no bedding (massive) and brecciated (Fig. 2). The two drill holes are separated by a horizontal distance of ~500 m. Lateral layer correlation appears very difficult based solely on the bedding. The thinly laminated layering, dominant in the Key Tuffite close to mineralization, appears to be a minor feature away from the mineralization. The bedding is not always well developed and previously unrecognized massive zones are dominant (Fig. 2b, e). The vertical variations proposed by Davidson (1977), based on the observations at Bell Allard South deposit, are not observed in these sections. From a mineralogical point of view, chert, considered to be by far the dominant component (up to 50 %) in the Key Tuffite (Davidson 1977; Liaghat and MacLean 1992), is present only locally. However, chlorite and sericite represent the dominant assemblage of the Key Tuffite. Finally, the base metal sulfides such as sphalerite and chalcopyrite are absent. These observations challenge the original perception of the Key Tuffite. Specifically, the well-developed layering, considered as the best evidence of component mixing (i.e. tuffaceous, hydrothermal: exhalative/alteration), disappears away from the mineralized lenses, questioning the origin and the source of the different components.

Geology of the Perseverance and Bracemac-McLeod deposits

Volcanic stratigraphy

The Perseverance and Bracemac-McLeod deposits are located at the most northern and southern ends of the south flank, respectively (Fig. 1a). The volcanic sequence of the south flank trends north-west with a variable dip towards the south-west. In the northern part (Perseverance area), the volcanic sequence is sub-horizontal with a shallow dip of 10° towards the south-west. The dip progressively increases going south-east to reach a maximum of 65° in the Bracemac-McLeod area. The general stratigraphic sequence is shown in Fig. 1b, whereas the detailed geology of both deposits is illustrated in the cross sections of Figs. 3 and 4. The lithological descriptions and main chemical characteristics of each unit are summarized in Table 1.

The Key Tuffite is well developed in the Perseverance and Bracemac-McLeod areas. Its thickness ranges between 0.1 and 10 m and in some places it is absent. Such variations can occur over short distances and make correlation of specific beds impossible. In addition, there is no systematic increase in the thickness of the Key Tuffite towards the deposits as previously documented around the Bell Allard South deposit (Davidson 1977), 2.2 km north-west of Bracemac-McLeod (Fig. 1).

At Perseverance, the Key Tuffite has a simple homogeneous facies, devoid of sulfides, which is dominated by alternating layers of silica and chlorite. Numerous soft sediment features, such as convoluted laminations, load and slump structures (Fig. 5f), are abundant in the Key Tuffite, which suggest important submarine tuffaceous sedimentation. In contrast, the Key Tuffite in the Bracemac-McLeod area contains a larger variety of facies composed of different amounts of quartz, chlorite, sericite, sulfides (mostly pyrite) and carbonate (Figs. 5a–e and 6). In the chert-rich facies, delicate lamination features are well preserved, whereas the bedding appears coarser in chlorite-rich facies.

In the vicinity of the Perseverance and Bracemac-McLeod deposits, the Key Tuffite is overlain by felsic rather than mafic units. At Perseverance, the felsic unit is the Dumagami rhyolite, which in fact has a rhyodacitic composition (Table 1). At Bracemac-McLeod, the felsic unit is the Bracemac rhyolite. This unit is very similar (in geochemical composition and in age) to the Watson rhyolite (Table 1). In turn, the Bracemac rhyolite is overlain by a thin exhalative unit: the Bracemac Tuffite which marks the transition into the andesitic rocks of the Wabassee Group. Most of the volcanic units in the lower part of the south flank (mine sequence) are tholeiitic except for the lower andesitic unit of the Wabassee Group which is transitional (Table 1).

At Perseverance, a large set of sub-vertical dykes of different orientations and compositions crosscuts the sub-horizontal volcanic strata, hence complicating the reconstruction of the succession (Fig. 3b, c). The orientation of the intrusions is different at Bracemac-McLeod where the entire stratigraphic succession has been intruded by gabbroic sills that inflate the volcanic pile (Fig. 4b, c).

Alteration, mineralization and their link with the Key Tuffite

The Perseverance and Bracemac-McLeod deposits are both surrounded by large (~1.6 km in diameter) alteration halos developed in the footwall Watson rhyolite (Figs. 3 and 4), which are characterized by a well-developed proximal chloritization (± talc), moderate intermediate chloritization and distal sericitization (Fig. 7). An alteration halo is also present in the overlying Bracemac rhyolite and Dumagami rhyodacite, although less extensive than in the footwall. In both deposits, the hanging wall alteration is dominated by

pervasive and patchy silicification and diffuse chloritization (Fig. 7a, b). Such alteration haloes are typical of Archean VMS systems (e.g. Galley 1993) and represent the main exploration tool (Large et al. 2001a). Despite similar alteration assemblages, the geometry of the alteration haloes and of the orebodies is markedly different at Bracemac-McLeod versus Perseverance (Figs. 3 and 4). Moreover, both are different to the classic mound-shaped lenses of exhalative VMS systems (e.g. Lydon 1988; Ohmoto 1996) as previously described in the Matagami Camp for the Mattagami Lake (Costa et al. 1983) and the Isle Dieu mines (Lavallière et al. 1994).

Perseverance deposit

The Perseverance deposit consists of three main sub-vertical lenses: Perseverance Main, Perseverance West and Equinox (Fig. 3a), which are thought to be spatially controlled by synvolcanic structures. Together, they contain 5.12 million tonnes with grades of 15.8 % Zn, 1.2 % Cu, 29 g/t Ag and 0.4 g/t Au (Arnold 2006). The three orebodies are preserved in a graben-like structure bounded by two north-west-trending faults (Arnold 2006; Bloom and Beaudry 2009). Most of the mineralization is present as sub-vertical massive sulfides

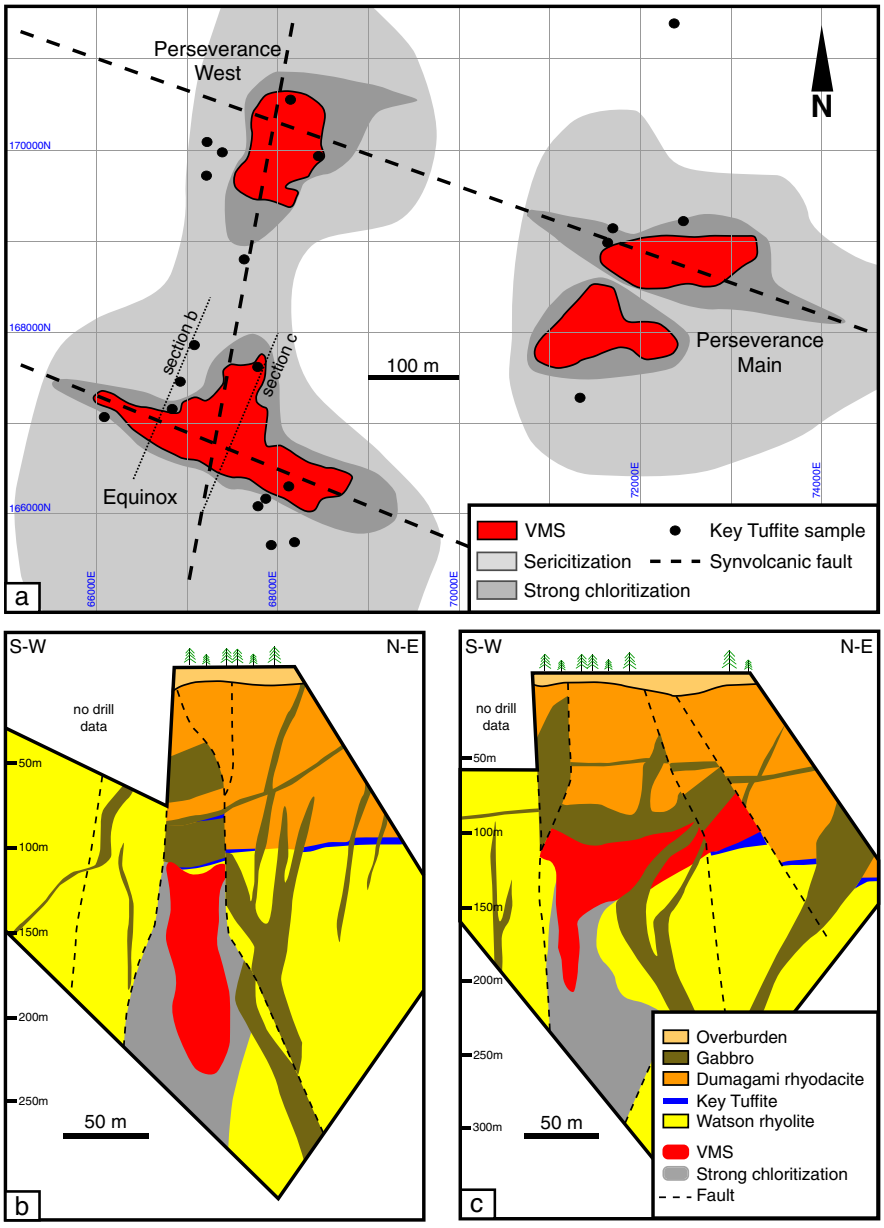

Fig. 3 Geology of the Perseverance deposit (modified from Glencore). **a** Plan view. **b**, **c** Cross section of the Equinox orebody

composed predominately of banded pyrite and sphalerite, with lesser amounts of chalcopyrite, pyrrhotite and magnetite hosted within the Watson rhyolite. A narrow (5 to 10 m thick) and sub-vertical intense chloritization (± talc) surrounds the mineralization (Fig. 3b, c). The sub-horizontal Key Tuffite, devoid of sulfides, systematically covers the mineralization (Fig. 3b, c). The only exception is at Equinox where sulfides are located above the Key Tuffite and appear to replace the Dumagami rhyodacite hanging wall (Fig. 3c). Underground observations (Figs. 8a, b and 9a) show that silicification and chloritization are also the dominant alteration styles in the Key Tuffite. Hydrothermal fluids have used the primary porosity of the hyaloclastic upper portion of the Watson rhyolite (Fig. 8a) or the structural porosity of synvolcanic fractures (Fig. 9a) to replace, in some cases totally, the primary textures. This silicification extends into the Dumagami rhyodacite hanging wall (Fig. 8b). The lack of mineralization in the Key Tuffite and the sub-vertical geometry of the orebodies, in a sub-horizontal stratigraphic pile, are unique in the Matagami mining camp. It is apparent from the cross sections (Fig. 3b, c) that the orebodies formed by replacement of the Watson rhyolite within synvolcanic structures, below the Archean seafloor. Moreover, both the alteration and mineralization are locally crosscutting the Dumagami rhyodacite hanging wall indicating that mineralization is mostly epigenetic in origin.

Bracemac-McLeod deposits

The Bracemac-McLeod mine consists of two deposits (Bracemac and McLeod) spatially controlled by synvolcanic faults and separated by a horizontal distance of 1,200 m (Fig. 4a). In contrast to the sub-vertical conduits of

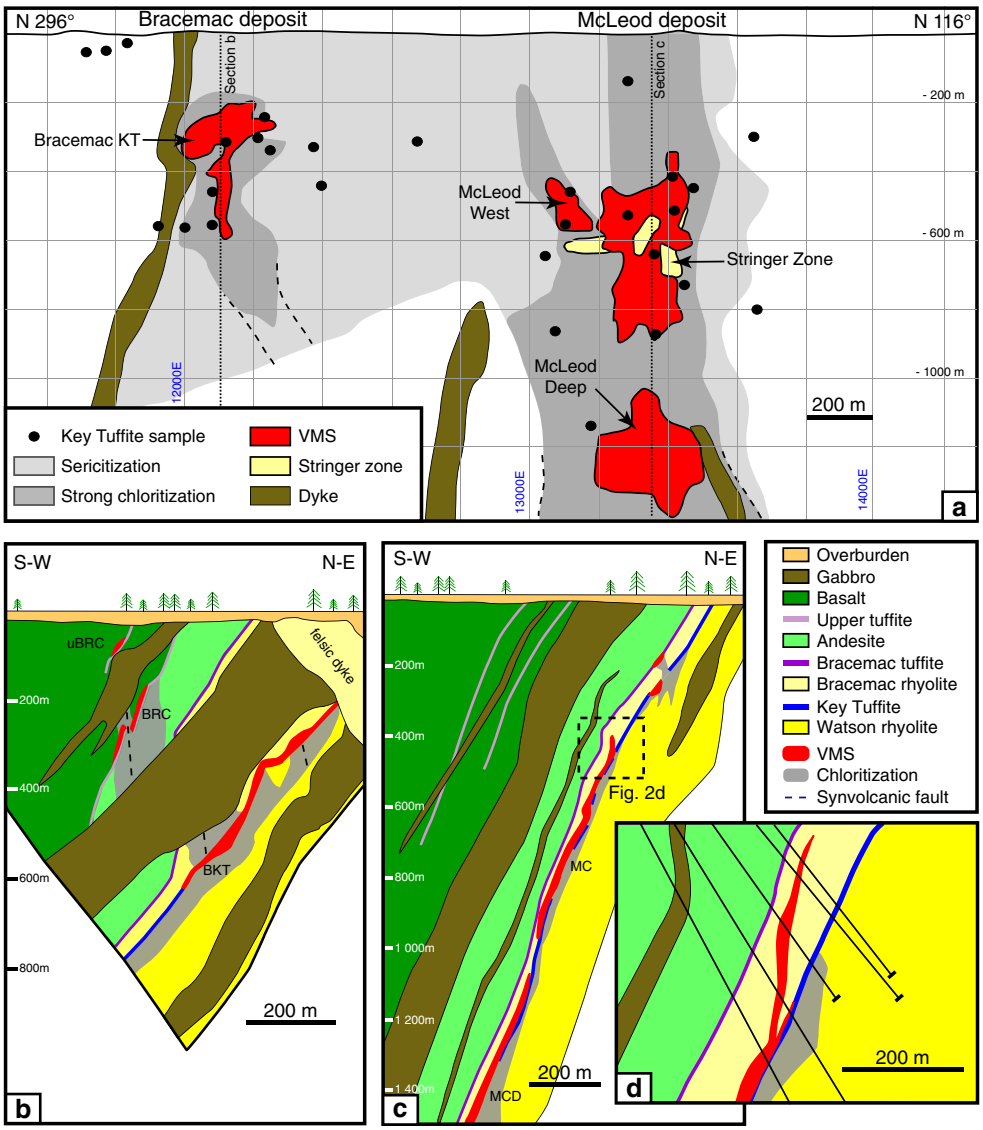

Fig. 4 Geology of Bracemac-McLeod deposits (modified from Donner Metals). **a** Composite longitudinal view. **b** Cross section of the Bracemac area. **c** Cross section of the McLeod area. *uBRC* Upper Bracemac, *BRC* Bracemac Main, *BKT* Bracemac KT

Table 1 Lithology descriptions and magmatic affinity (Barrett and MacLean 1999) of the volcanic sequence at Bracemac-McLeod and Perseverance. Geochemical ratios are calculated with a compilation of data from the Glencore database, Debreil (personal communication) and this study

	Mineralization	Lithology	Code	Short description	Thickness (m)	Alteration features	Zr/TiO_2* 10000	Zr/Y	La/Yb	Affinity
Wabassee Group	uBRC	Basalt	V3B	Dark green, aphanitic to glomeroporphyric lavas Massive, pillowed, pillow-breccia and hyaloclastites	> 400	Moderate chloritization and pyritization of pillow margins	0.01	2.00	2.31	Tholeiitic
	BRC	Upper Tuffite	UT	Thinly layered, mafic	0.1 to 2	Chloritization and pyritization	-	-	-	-
		Andesite	V2J	Light green, fine grained lavas Massive, pillowed, pillow-breccia and	~120	Moderate chloritization and pyritization of pillow margins	0.01	4.00	2.80	Transitional
Watson Group		Bracemac Tuffite	BT	Thinly layered chert, pyrite and mafic ash	0.2 to 0.3	Silicification and pyritization		-	-	-
		Bracemac Rhyolite	BRV1B	Grey to dark grey fine-grained lavas 1 to 5% of 1-3mm quartz phenocrysts Mostly massive	25 to 60	Proximal: Strong pervasive silicification Local sericitization	0.2	2.77	1.96	Tholeiitic
	BKT, MC, MCW, MCD	Key Tuffite	KT	Thinly layered mafic ash	0.1 to 10	Silicification, chloritization, sericitization, pyritization. Highly variable	0.03	10.39	10.44	Calc-alkaline
Watson Group	SZ	Watson Rhyolite	WV1B	Grey to dark grey fine-grained lavas 1 to 5% of 1-3mm quartz phenocrysts Massive, lobes but rare breccias Upper part often hyaloclastite	~200	Proximal: Strong black chloritization and talc; Distal: moderate chloritization and sericitization; Local silicification	0.2	4.10	2.14	Tholeiitic
		Bell River Complex	BC	Gabbro-anorthosite layered intrusion	~5000		-	-	0.96	Tholeiitic

Bracemac-McLeod

Wabassee Group		Dumagami Rhyodacite	DV1B	Grey to dark grey fine-grained lavas Up to 90% spherulites (1-5mm) Massive, rare volcanic textures	> 400	Proximal: Strong black chloritization and talc; Distal: moderate chloritization and sericitization; Local silicification	0.06	3.55	-	Tholeiitic
	EQ	Key Tuffite	KT	Thinly layered mafic ash	0.1 to 10	Strong silicification, moderate chloritization, barren of sulfides	0.03	10.39	10.44	Calc-alkaline
Watson Group	PER, PW	Watson Rhyolite	WV1B	Grey to dark grey fine-grained lavas 1 to 5% of 1-3mm quartz phenocrysts Massive, lobes but rare breccias Upper part often hyaloclastite	~200	Proximal: Strong black chloritization and talc; Distal: moderate chloritization and sericitization; Local silicification	0.2	4.1	2.14	Tholeiitic

Perseverance

uBRC Upper Bracemac, *BRC* Bracemac, *BKT* Bracemac KT, *MC* McLeod, *MCW* McLeod West, *MCD* McLeod Deep, *SZ* Stringer Zone, *EQ* Equinox, *PER* Perseverance Main, *PW*> Perseverance West

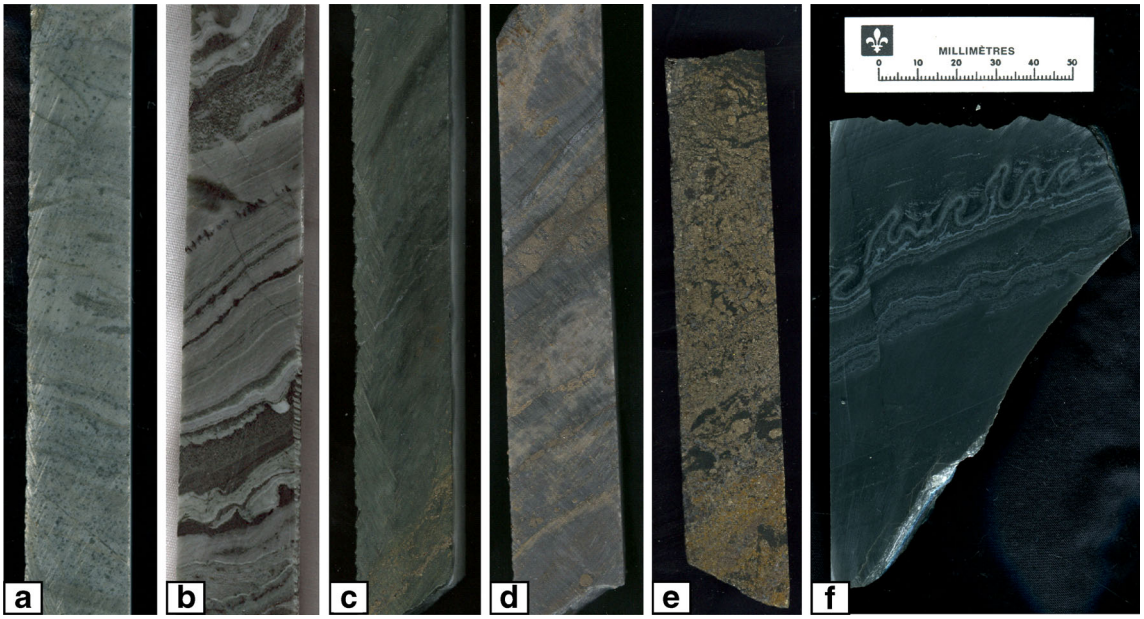

Fig. 5 Representative mineral assemblages of selected Key Tuffite samples around Bracemac-McLeod (**a**–**e**; core width=2.4 cm) and Perseverance (**f**) to illustrate the variation in facies. **a** Silica-sericite (sample 972209 in drill hole BRA-09-06, 85 m depth). **b** Silica–chlorite (716472 in BRC-08-76, 692 m). **c** Chlorite–pyrite (972162 in MC-08-62, 585 m). **d** Silica–sericite–pyrite (972116 in MC-08-55, 513 m). **e** Pyrite–chlorite (972153 in MC-07-23, 519 m). **f** Chlorite–silica (969357, level 105-PS26, underground)

Perseverance, the Bracemac-McLeod orebodies are sheet-like and sub-parallel to the volcanic stratigraphy that dips 55–65° to the south-west. The Bracemac deposit (Fig. 4b) comprises three distinct lenses, Bracemac KT, Bracemac Main and Upper Bracemac. They form a stacked sequence connected by a chlorite/sulfide alteration structure, which could be interpreted as resulting from the reactivation of a hydrothermal system along a synvolcanic structure after the deposition of the Wabassee Group (Adair 2009). It is one of the first occurrences of stacked mineralization found in the Matagami Camp. The McLeod deposit is composed of four lenses: McLeod Zone, Stringer Zone, McLeod West and the newly

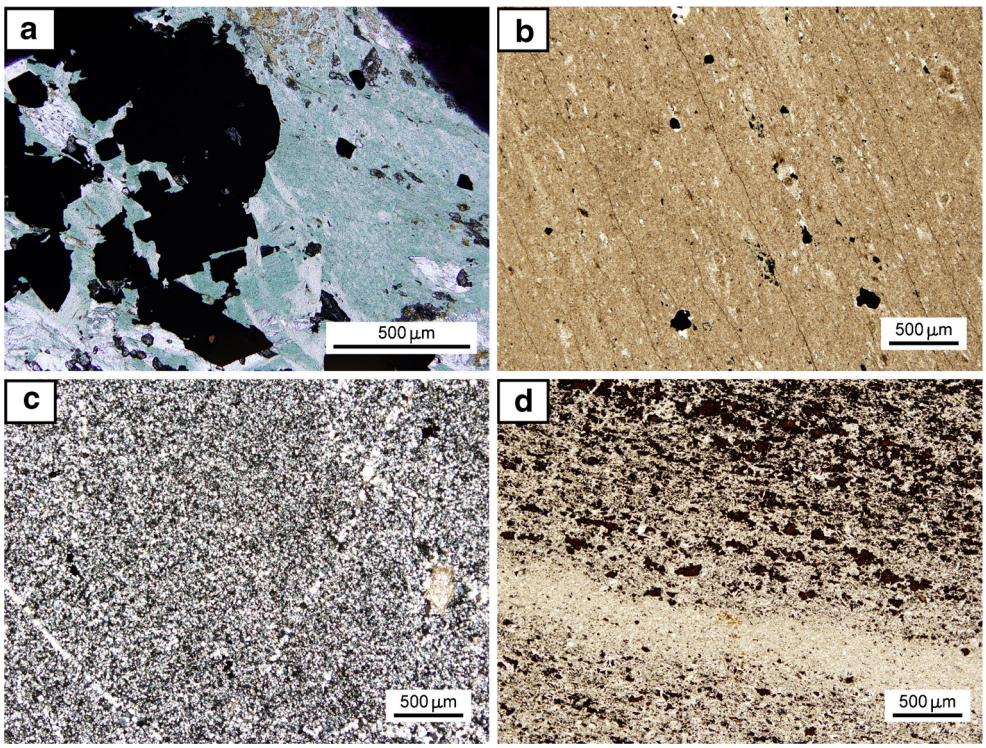

Fig. 6 Photomicrographs of the Key Tuffite. Dominant assemblages: **a** Chlorite and pyrite (plane-polarised light = ppl) around McLeod (972110 in MC-07-24, 686 m). **b** Sericite (ppl) around McLeod (716474 in MC-05-19, 821 m). **c** Quartz (cross-polarized light) around McLeod (716489 in MC-05-18, 928 m). **d** Disseminated sphalerite in a chlorite/sericite-rich Key Tuffite (ppl) around Bracemac (972134 in BRC-95-11, 968 m)

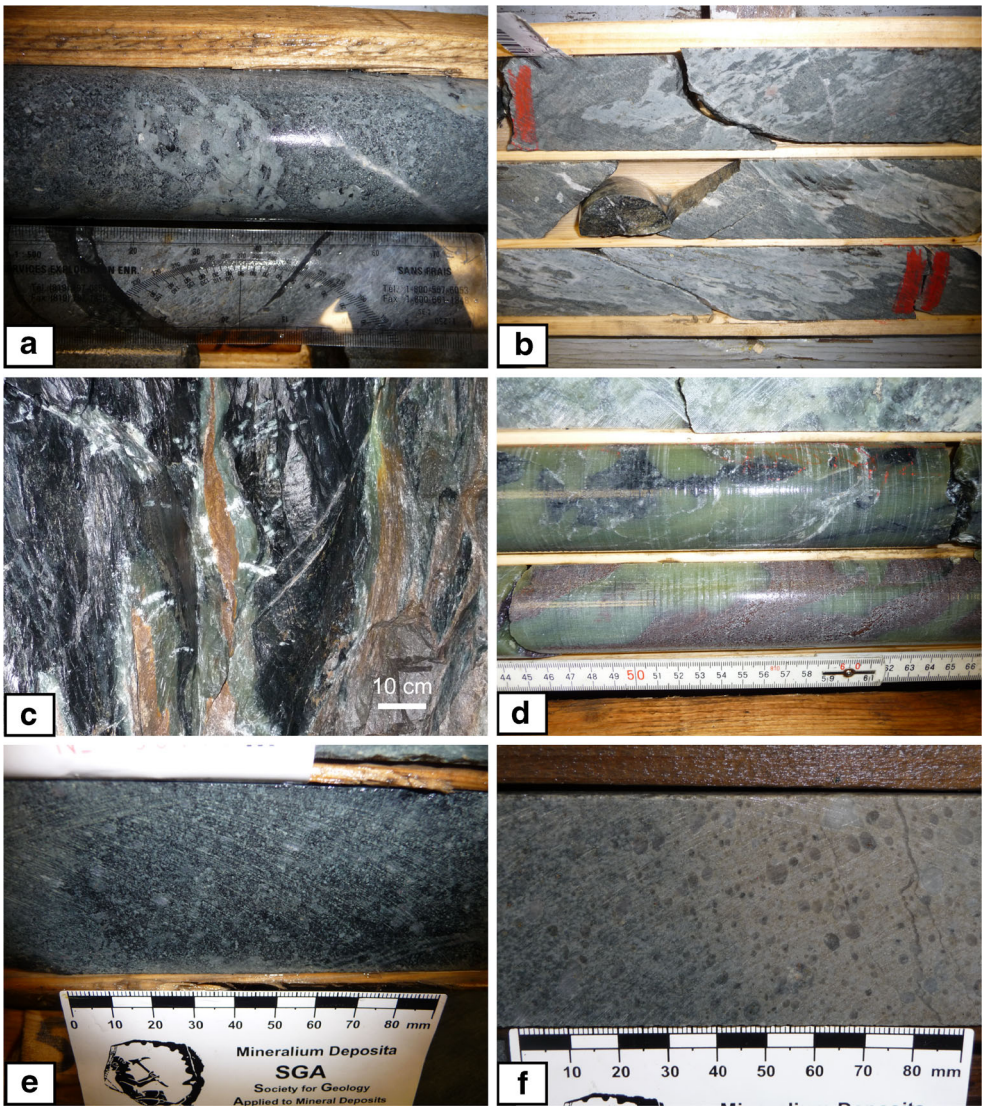

Fig. 7 Variability in the alteration assemblages at Perseverance and Bracemac-McLeod deposits. **a** Patchy silicification in the Dumagami rhyodacite at Perseverance (PER-00-54, 74 m). **b** Patchy and pervasive silicification in the Bracemac rhyolite at McLeod (MC-10-92A, 466 m). **c** Talc and sphalerite stringers in the Watson rhyolite at Perseverance (underground). **d** Strong proximal talc ± chlorite alteration in the Watson rhyolite at Bracemac (BRC-09-152, 546 m). **e** Black chloritization of the Watson rhyolite at McLeod (MC-04-04, 530 m). **f** Distal sericitization of the Watson rhyolite at Bracemac (BRC-07-45, 480 m)

discovered McLeod Deep. Apart from the Stringer Zone, which is hosted in the Watson rhyolite, they all occur at the Key Tuffite level. Altogether, the Bracemac-McLeod deposits contain measured and indicated mineral resources of 3.6 million tonnes grading 10.6 % Zn, 1.5 % Cu, 32 g/t Ag and 0.5 g/t Au (Côté and Lavigne 2010). Additional inferred mineral resources of 2.6 million tonnes grading 8.8 % Zn, 1.3 % Cu, 38.8 g/t Ag and 1.1 g/t Au are present in and around the McLeod Zone, including the McLeod Deep lens discovered in 2010 (Côté and Lavigne 2010). Geometrically, the extensive and thin stratiform mineralization (~1.6 km and still open at depth by ~250 m, <20 m thick) of the McLeod deposit along the Key Tuffite unit (Fig. 4c) is also divergent from the classic mound-shaped lens model of the Matagami mining camp. The mineralogy of both deposits is dominated by pyrite and sphalerite with lesser amounts of chalcopyrite and pyrrhotite (± magnetite and minor galena). The strong chlorite alteration halo is limited to 50 m stratigraphically below the mineralization, but widespread over 1.6 km along dip (Fig. 4). Drill core observations of the Bracemac-McLeod deposits clearly demonstrate that a significant portion of the mineralization crosscuts and locally replaces the following units: (1) the Key Tuffite unit (Figs. 8c and 9b), (2) the hyaloclastic deposits in the uppermost portion of the footwall Watson rhyolite (Fig. 8d) and (3) the Bracemac rhyolite hanging wall (Fig. 4c). In the uppermost portion of the McLeod Zone, the majority of the massive sulfide lens is hosted in the Bracemac rhyolite hanging wall (Fig. 4d), whereas at depth, it is associated with, or immediately below, the Key Tuffite unit. Genetically, these relationships are not easily reconcilable with an exhalative origin of mineralization on the seafloor, although it can still be argued that the mineralizing event continued after the seafloor covering by the Bracemac rhyolite, as demonstrated by the stacking at Bracemac and McLeod. However,

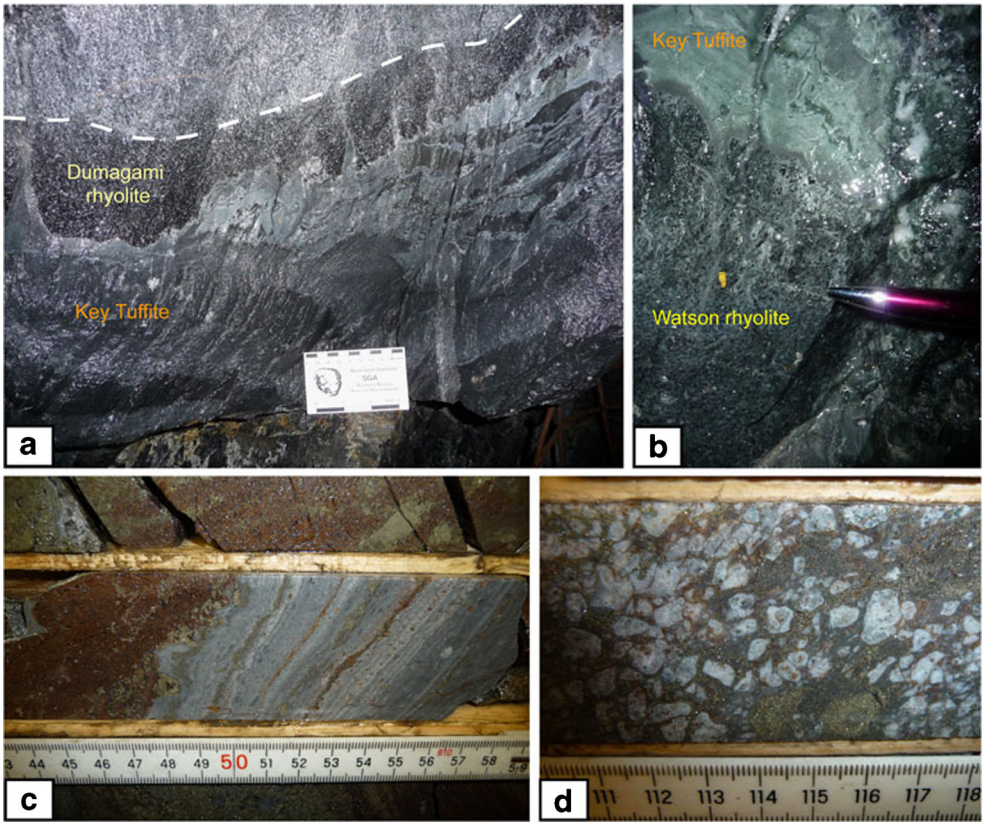

Fig. 8 Drill core and underground photographs illustrating the link between Key Tuffite, alteration and mineralization at Perseverance (**a**, **b**) and Bracemac-McLeod (**c**, **d**). **a** Silica-rich Key Tuffite and silicification and chloritization of the lower part of the Dumagami rhyodacite (Equinox, underground, level 105-PS26). **b** Silicification of the hyaloclastic summit of the Watson rhyolite (Equinox, underground, level 105-PS26). **c** Silicified Key Tuffite enclaved in the massive sulfide zone of Bracemac KT (BRC-09-124, 318 m). **d** Progressive replacement by sphalerite and pyrite of the hyaloclastic summit of the Watson rhyolite at Bracemac (BRC-09-124, 320 m)

within the Key Tuffite unit, both the relative position and textures of the mineralization are highly variable. The silicification and the mineralization commonly crosscut and replace the Key Tuffite bedding (Figs. 8c and 9b) and can occur at any stratigraphic level within the Key Tuffite, from the upper to the lower contact. These features are not expected for exhalative systems, but are more consistent with a replacement origin (Doyle and Allen 2003). Based on all the crosscutting, replacement and geometric relationships, it is considered that the epigenetic component of the VMS system was the dominant process in forming the mineralization at Bracemac-McLeod.

Chemical characterization of the Key Tuffite

Sampling and methodology

A total of 67 samples of the Key Tuffite, from 48 drill holes, were collected from the surrounding area of Perseverance and Bracemac-McLeod. The position of the samples is illustrated on Figs. 3a and 4a. For comparison, an additional six drill holes (nine samples), located away from all known mineralization (>450 m), were also selected at the scale of the mining camp. Whole-rock geochemistry was carried out on 76 samples of Key Tuffite (20 cm in length) for major, trace and rare earth elements (REE) at the INRS laboratory in Quebec City, Canada. A metaborate fusion was carried out on all samples, prior to inductively coupled plasma-atomic emission spectrometry and mass spectrometry (ICP-MS) analyses, for a total dissolution of resistant minerals. Standards were used to monitor the accuracy (within 10 % relative difference) and reproducibility (<10 % relative standard deviation) of the analyses (Electronic Supplementary Material). Supplementary Key Tuffite data (n =25) from Perseverance, analysed by Glencore at ALSChemex laboratory (Canada), were integrated into our database. Results for major, trace and rare earth elements for all samples are given in the "Electronic Supplementary Material". Table 2 presents average concentrations and standard deviation for selected major, trace elements and REE in the Key Tuffite samples from the Perseverance, Bracemac-McLeod deposits and from samples located away from known mineralization.

The composition of individual millimetric layers was analysed by laser ablation (LA) ICP-MS at the University of Quebec at Chicoutimi (UQAC), Canada, in order to investigate the origin of the layering of the Key Tuffite. The methodology follows the one described by Baldwin et al. (2011) developed for in situ analyses of chert microbands in iron formations. The results, standards and details on the method are also presented in the "Electronic Supplementary Material".

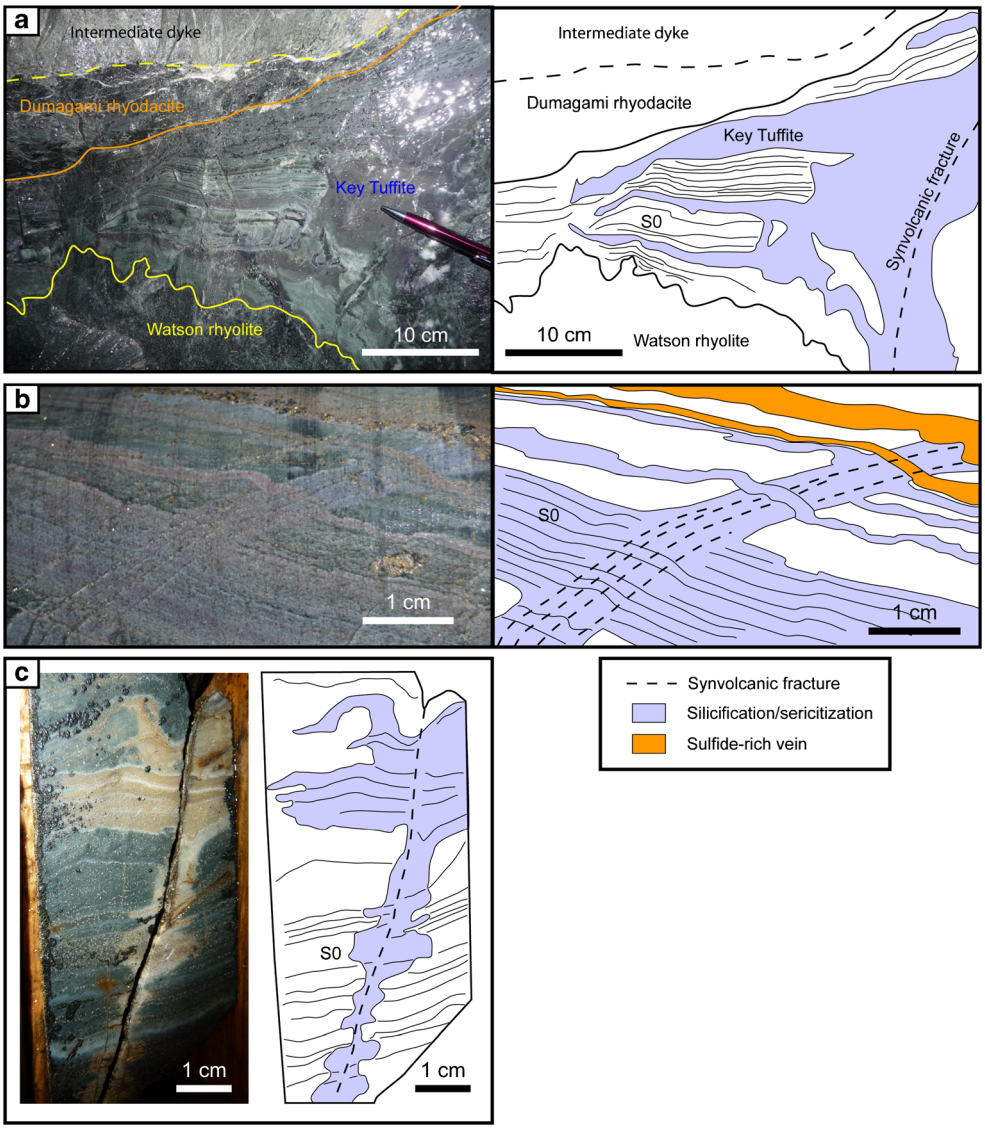

Fig. 9 Alteration and replacement of specific layers in the Key Tuffite. **a** Strong silicification of the Key Tuffite at Perseverance (Equinox, underground, level 105-PS26). **b** Selective silicification at Bracemac (BRC-97-15, 1207 m). **c** Selective silicification/sericitization at Orchan (IM-87-85, 869 m)

Tuffaceous component

The characterization of the tuffaceous component is critical to understand the petrogenesis of the Key Tuffite. Furthermore, this component has the potential to dilute the hydrothermal component (i.e. exhalative and/or alteration). The identification of the tuffaceous source/s can only be approached by the use of immobile elements. In VMS systems, most of the major and many of the trace elements are mobile during hydrothermal alteration (Barrett and MacLean 1999). Only TiO_2 and Zr are considered immobile even during extreme alteration (Finlow-Bates and Stumpfl 1981). Thus, the ratio of these two elements is commonly used to discriminate altered rocks in volcanic terranes (e.g. MacLean and Kranidiotis 1987; Barrett et al. 2005).

Figure 10a represents a plot of immobile elements for all the volcanic rocks around the Bracemac-McLeod and Perseverance area. Although the absolute TiO_2 and Zr values are highly variable, the ratios remain constant for each lithology and plot along different alteration lines through the origin. The $Zr/(TiO_2 \times 10{,}000)$ ratios of the Bracemac and Watson rhyolites (0.2) are an order of magnitude higher than those of the Wabassee andesite (0.01) and Key Tuffite (0.03) (Table 1). The Key Tuffite was interpreted by Liaghat and MacLean (1992) to be a mixture of andesitic calc-alkaline (Wabassee Group) and rhyolitic tholeiitic material (Watson Lake Group). However, the Key Tuffite is clearly different in composition from the underlying Watson rhyolite and overlying Bracemac rhyolite (Fig. 10a) suggesting a negligible input of rhyolitic ash. In addition, the samples plot along a line passing through the origin with correlative values for Pearson product of 0.90 and R^2 of 0.81 for these immobile elements (Fig. 10). Such a sample

Table 2 Median compositions of the Key Tuffite around the Perseverance and Bracemac-McLeod deposits and calculated precursor

%	Chlorite Zone Bracemac-McLeod		Chlorite Zone Perseverance		Sericite Zone Bracemac-McLeod		Calculated precursor >450 m	
	n=37		*n*=47		*n*=8		*n*=9	
	Average	σ	Average	σ	Average	σ	Average	σ
Loi	5.80	3.22	5.10	2.01	4.47	1.12	5.26	2.52
Al_2O_3	9.21	4.59	10.51	4.18	12.75	2.76	15.22	1.60
CaO	0.86	1.43	0.47	1.32	1.41	1.18	2.75	2.06
Fe_2O_3T	15.64	9.38	7.21	3.12	9.02	2.33	9.47	3.22
K_2O	1.59	1.64	0.20	0.35	3.22	1.85	2.77	0.95
MgO	2.66	1.40	9.45	3.61	2.05	1.57	1.85	0.67
MnO	0.11	0.12	0.05	0.03	0.06	0.02	0.09	0.05
Na_2O	0.13	0.40	0.32	0.72	0.70	0.81	3.40	1.58
P_2O_5	0.07	0.04	0.07	0.08	0.09	0.03	0.10	0.03
SiO_2	60.92	12.92	65.80	10.57	63.72	4.88	56.12	7.29
TiO_2	0.33	0.16	0.39	0.17	0.46	0.09	0.51	0.07
ppm								
Zr	86.75	41.10	93.10	35.66	123.65	34.49	123.21	22.53
Nb	3.44	1.64	3.79	1.79	4.99	1.28	5.59	2.78
La	10.22	7.20	8.30	4.97	16.75	8.07	12.03	3.88
Ce	22.63	16.26	18.01	10.58	37.86	17.25	26.56	8.44
Pr	2.91	2.14	2.22	1.24	4.84	2.27	3.28	1.15
Nd	11.60	9.67	9.27	5.00	20.94	9.62	12.76	4.69
Sm	2.87	2.58	2.18	0.93	5.08	2.73	2.59	0.95
Eu	0.99	0.58	0.62	0.25	1.01	0.33	0.80	0.28
Gd	2.86	2.39	2.00	0.79	4.91	2.75	2.51	1.10
Tb	0.42	0.38	0.28	0.12	0.73	0.40	0.33	0.14
Dy	2.56	2.49	1.72	0.72	4.31	2.22	2.01	0.67
Y	18.40	19.36	11.18	8.11	26.66	14.01	11.94	4.33
Ho	0.54	0.58	0.35	0.14	0.87	0.45	0.39	0.13
Er	1.54	1.55	1.02	0.39	2.40	1.12	1.16	0.33
Tm	0.22	0.22	0.15	0.05	0.35	0.15	0.17	0.05
Yb	1.40	1.29	1.03	0.34	2.18	0.85	1.17	0.32
Lu	0.21	0.19	0.15	0.05	0.33	0.12	0.17	0.05
ΣREE	60.97	44.17	47.30	23.81	102.56	47.07	65.93	21.84

distribution clearly indicates that the composition of the tuffaceous component was a homogeneous ash prior to mass gain and loss induced by hydrothermal alteration. If different sources were involved in the formation of the Key Tuffite, a much wider dispersion and/or different slopes of the alteration lines would be expected on the immobile element plots. The similarity of the alteration lines between the Key Tuffite and the andesitic unit of the hanging wall Wabassee Group (Fig. 10a) and a plot of Nb/Y versus Zr/TiO_2 (Fig. 10b) indicates an andesitic composition of the Key Tuffite. The dispersion of samples along the Nb/Y axis indicates that Y was not entirely immobile, as already demonstrated by Finlow-Bates and Stumpfl (1981) in VMS environments.

In order to establish the tuffaceous component composition prior to hydrothermal alteration, the unaltered precursor was calculated using an average of nine samples from five drill holes located more than 450 m away from any known deposit. Two of these nine selected Key Tuffite sections are presented in Fig. 2. Geochemical data confirm the homogeneous composition for the major (Fig. 11a), trace (Fig. 11b) and rare earth elements (Fig. 11c) highlighting the absence of vertical geochemical variation despite the textural diversity. The alteration box plot (Large et al. 2001b), used as an

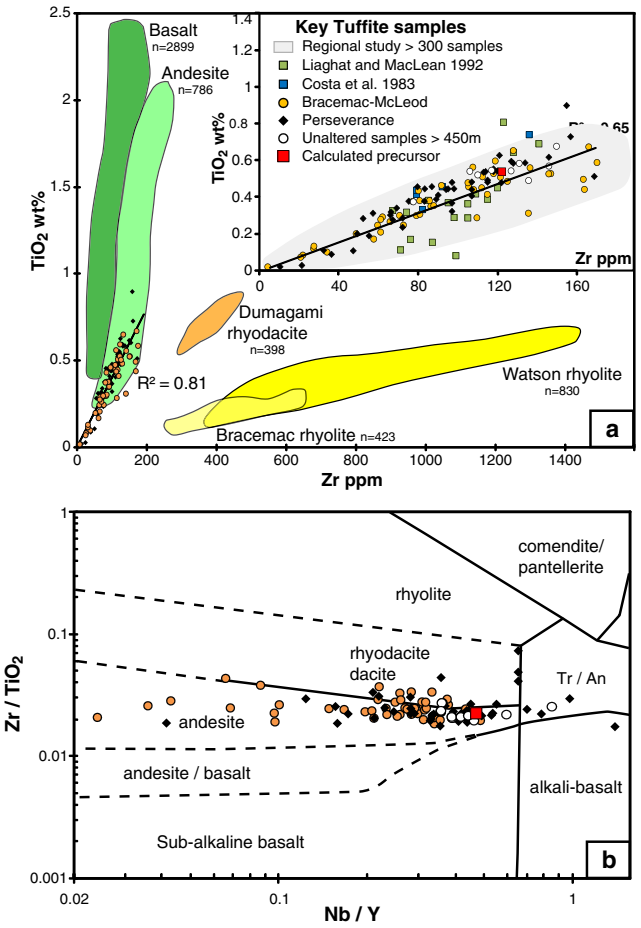

Fig. 10 Whole-rock geochemistry of the volcanic rocks of Matagami. **a** In Zr versus TiO_2, fields represent the different lithologies and are based on the Glencore geochemical database. *Inset*: Key Tuffite data compilation from Genna (unpublished). **b** Zr/Ti versus Nb/Y diagram of Winchester and Floyd (1977)

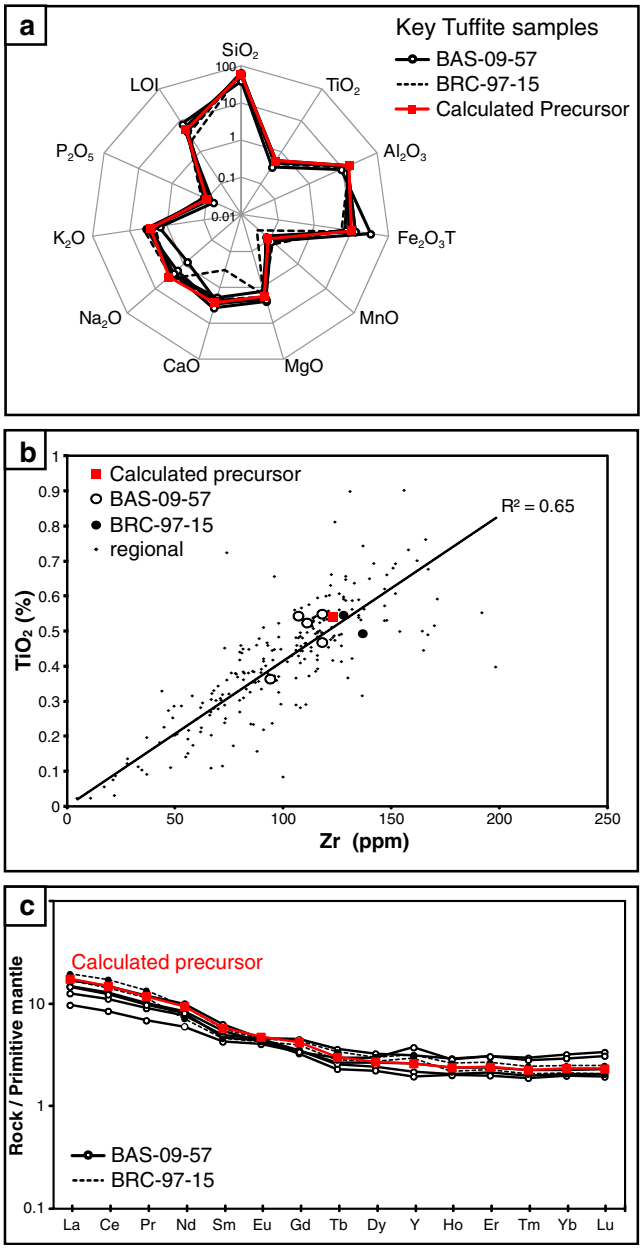

Fig. 11 Detailed geochemistry of the Key Tuffite away from the mineralization (>1 km) from the two drill holes (BAS-09-57 and BRC-97-15; Figs. 1 and 2). **a** Spidergram for the major elements. **b** Zr versus TiO_2. **c** REE-Y multi-element variation diagrams normalized to primitive mantle values from Sun and McDonough (1989)

external validation, confirms the minimal chemical change undergone by the nine samples selected for the precursor calculation (Fig. 12). As expected, the selected samples plot within the field of unaltered andesite established by Gemmell and Fulton (2001). All the other samples from around the Perseverance and Bracemac-McLeod deposits, except one, are extremely altered and plot toward the chlorite pole. The arithmetic average of the composition of these nine samples is considered to represent the initial precursor and thus the tuffaceous component composition (Table 2).

The REE are also generally considered as immobile and consequently are widely used for establishing volcanic stratigraphic successions (MacLean 1988; Barrett et al. 2005) and source determination for sedimentary rocks (Bierlein 1995). As shown in Fig. 13a, the Key Tuffite has a different REE-Y pattern to the Bracemac and Watson rhyolites and is closer in composition to the Wabassee mafic units. Taking into account the REE-Y content and the La/Yb and Zr/Y ratios (Table 1), the best candidate matching the Key Tuffite composition is the lower andesitic unit of the Wabassee. This unit directly overlies the Key Tuffite along most of the south flank, but not at Bracemac-McLeod and Perseverance (Figs. 3 and 4). Figure 13b compares the REE-Y content of the unaltered Key Tuffite samples with the Wabassee andesite. Despite the similarity in the REE-Y values, unaltered Key Tuffite samples have a slightly more fractionated pattern compared to the andesite.

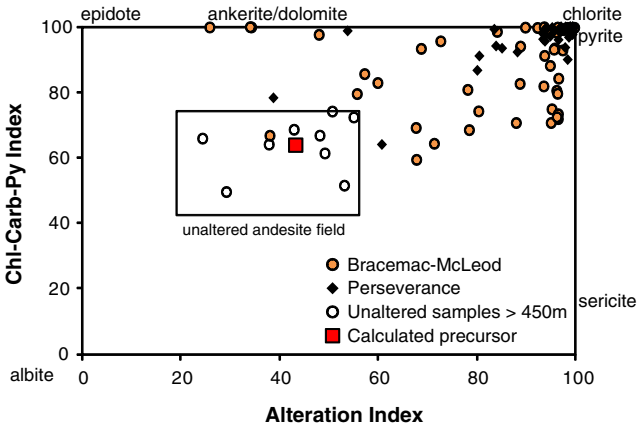

Fig. 12 Alteration box plot for the Key Tuffite samples (modified from Large et al. (2001b). *AI* Ishikawa alteration index, *CCPI* chlorite–carbonate–pyrite index

Hydrothermal component

In order to calculate the hydrothermal effect on the tuffaceous precursor, a mass change calculation was used, based on the MacLean and Kranidiotis (1987) single precursor approach. The gain or loss of an element was calculated by subtracting the reconstituted value of the mobile element in the altered sample from that in the precursor. The general equation, using SiO_2 as an example and TiO_2 as the immobile monitor, is as follows:

$$\Delta SiO_2 = (TiO_2\,\text{precursor}/TiO_2\,\text{sample} \times SiO_2\,\text{sample}) - SiO_2\,\text{precursor}$$

The results are expressed in terms of mass change in weight percent (Δ).

Figure 14 represents the results of the mass change calculation for the major elements as a function of the distance toward the Bracemac-McLeod and Perseverance deposits. The composition far from the deposit is homogeneous with minimal alteration until 230 m from the mineralization. From this point toward the deposits, the composition systematically increases for most elements (except K_2O and Na_2O). In particular, ΔFe_2O_3 and ΔMgO represent a strong chloritization halo about 230 m around Perseverance and Bracemac-McLeod. Despite the similar general increase of these two elements towards the mineralization, the behaviour of Fe_2O_3 and MgO in the vicinity of the two deposits (last 100 m) is different. At Perseverance, ΔFe_2O_3 is significantly lower than that at Bracemac-McLeod (median of −0.9 % compared to 16.5 %, respectively). This is explained by the lack of sulfides (pyrite) in the Key Tuffite overlying the mineralization at Perseverance. In contrast, ΔMgO is higher at Perseverance than at Bracemac-McLeod (median of 12.1 % against 2.2 %) due to a greater abundance of talc in the alteration halo at Perseverance. Based on petrographic examination (Fig. 6b), sericite appears to be the only K-bearing hydrothermal mineral phase; therefore, the ΔK_2O is interpreted to reflect the distribution of sericite alteration. Mass gain of K_2O (up to 3.2 %) occurs between 400 and 230 m and represents a strong sericite alteration. The uniform depletion of Na_2O closer than 400 m (median of −3.5 %) illustrates the breakdown of plagioclase during sericitization (e.g. Eastoe et al. 1987). Then, mass loss of K_2O (up to −2.9 %) is dominant between 230 and 20 m, apart from one anomalous sample, and illustrates the classic VMS alteration transition by breakdown of sericite to form chlorite (e.g. Sangster 1972; Lydon 1988; Large 1992; Large et al. 2001b). Finally, both mass gain and loss in K_2O are recorded in the Key Tuffite in the last 20 m around the mineralized lenses. The more restricted sampling around the Perseverance deposit (only two samples between 200 and 400 m) does not allow the observation of the same pattern.

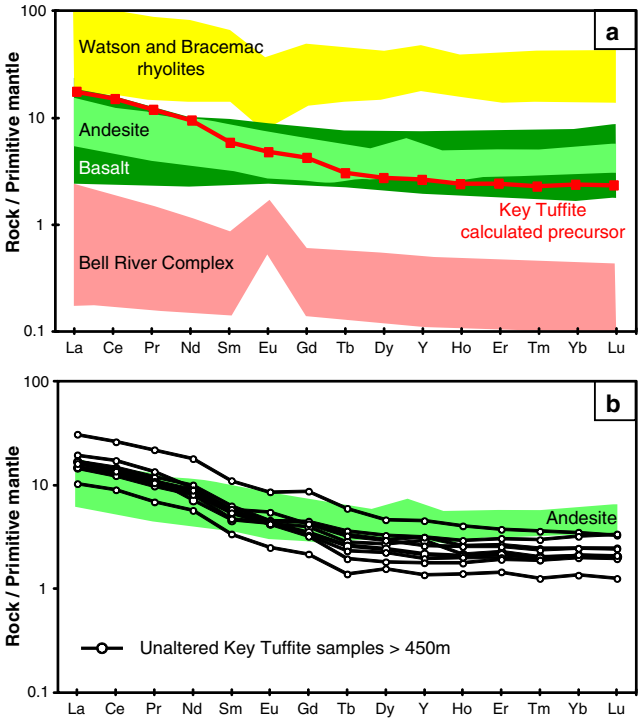

Fig. 13 REE-Y multi-element variation diagrams normalized to primitive mantle values from Sun and McDonough (1989). **a** Volcanic rocks of Matagami. Fields are from Gaboury and Pearson (2008), Piché (1991), Munoz Taborda (2011), Maier et al. (1996) and Debreil (personal communication). **b** Comparison between unaltered Key Tuffite samples and the lower andesitic unit of the Wabassee. Field from Debreil (personal communication)

Significance of layering

The finely developed layering in the Key Tuffite was previously presented as evidence for component mixing of variable tuffaceous sources (Liaghat and MacLean 1992) and exhalative chemical precipitates (Davidson 1977). The

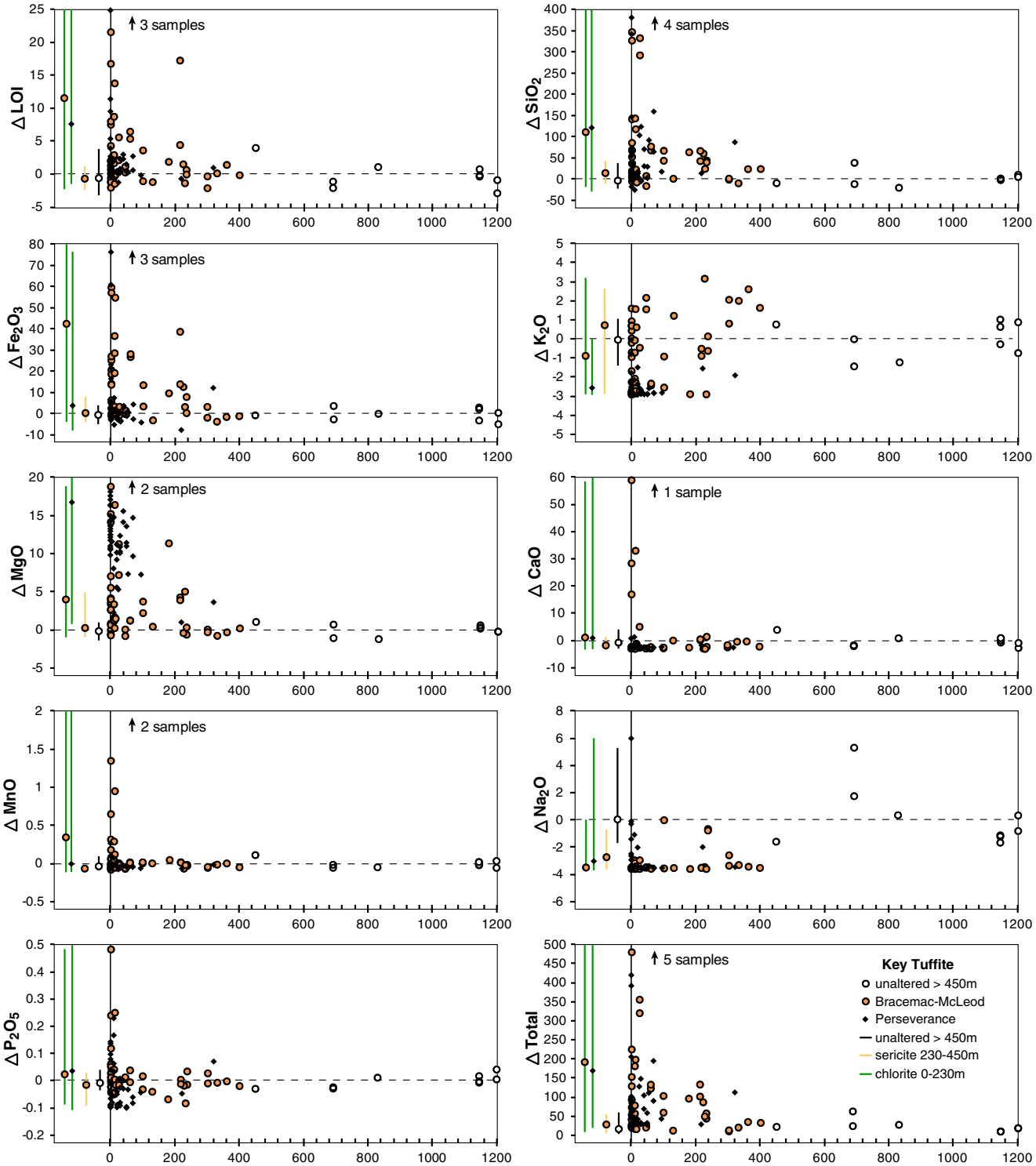

Fig. 14 Mass balance calculation for the major elements versus distance towards Bracemac-McLeod and Perseverance deposits. The *bar graph on the left-hand side* of each diagram gives the minimum, maximum and median values for both Perseverance and Bracemac-McLeod deposits and for each alteration facies

layering is particularly well developed in the Key Tuffite at Perseverance (Figs. 5f and 15) and together with the absence of sulfide implies that it was preserved from later modification by epigenetic mineralization. This portion is thus considered as the best candidate for testing (1) mixing of ash and (2) a possible low temperature chemical silica precipitate. A total of eight lines from three zones (Fig. 14 and "Electronic Supplementary Material") were ablated by LA-ICP-MS: six represent different

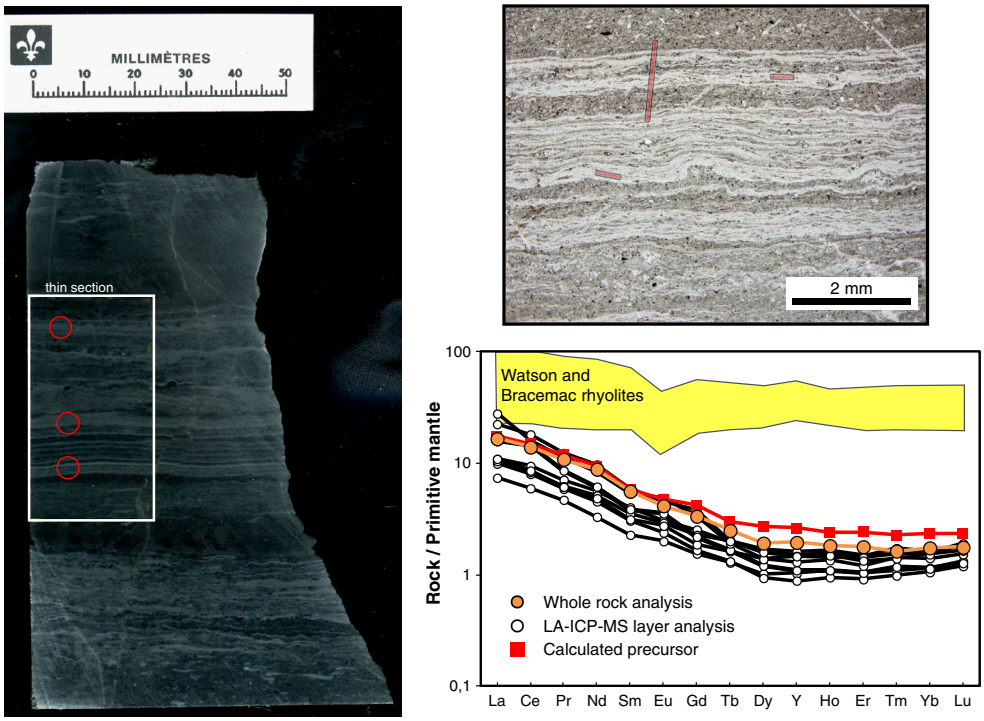

Fig. 15 In situ LA-ICP-MS analyses in a Key Tuffite sample from Perseverance mine (969352, Equinox, underground, level 105-PS26). *Red lines* on the microphotograph are laser ablation lines

silica-rich layers and two are perpendicular to layering (i.e. including chlorite and silica-rich layers). Results show that REE-Y patterns are very similar to each other, regardless of their silicic or chloritic composition, and are very similar to the composition of the corresponding whole-rock analysis (Fig. 11a). A distinctive felsic ash contribution accounting for the silicic layers can be discarded, as REE patterns are not similar to whole-rock pattern of rhyolites. Furthermore, the similarity of REE patterns from silicic to chloritic layers is more compatible with a silicification overprint of a homogeneous andesitic layered tuffaceous rock rather than that of ash and exhalative chemical precipitate mixing. Therefore, the in situ LA-ICP-MS results confirm the homogeneous andesitic composition of the Key Tuffite.

Discussion

Origin of the Key Tuffite

Tuffaceous component

Liaghat and MacLean (1992) investigated the parental tuffaceous component. They proposed, with a limited number of samples (Fig. 10a, inset), that the tuffaceous component resulted from mixing calc-alkaline andesite and tholeiitic rhyolite ashes in various proportions. The distinction of these two endmember sources was based on wide variation of the LREE-Y values and variable slopes of alteration lines (Fig. 7a, b of Liaghat and MacLean 1992). Instead, our larger database indicates that the Key Tuffite unit, on the south flank of the Matagami district, is andesitic in composition (Fig. 10) with a calc-alkaline affinity (Table 1). The composition prior to hydrothermal alteration was homogeneous as shown by a Pearson product of 0.90 with a R^2 of 0.81 for the immobile elements (Zr-TiO_2, Fig. 10a). Furthermore, data from Liaghat and MacLean (1992) also yield a Pearson product of 0.82 with a R^2 of 0.67 indicating, in combination with data from previous studies (Fig. 10a, inset), that the Key Tuffite unit is not the result of volcanic ash mixing. This is confirmed not only by our regional study (Genna, unpublished) on more than 300 whole-rock analyses from the whole mining camp (Fig. 10a, inset), but also by the LA-ICP-MS analyses at the scale of the thin section (Fig. 15).

The lower andesitic unit of the Wabassee Group directly overlies the Key Tuffite over most of the south flank, except in the Perseverance and Bracemac-McLeod areas (Fig. 1). The stratigraphic position and the similarity in composition (Fig. 10a) of the Key Tuffite with this andesite suggest a genetic link. The andesite represents the logical effusive equivalent of the Key Tuffite and is the best candidate for the source of the tuffaceous component of the Key Tuffite. The only other alternative would be a hypothetical unknown source from outside the Matagami volcanic succession. However, despite the similarity in the REE-Y values (Fig. 13b), unaltered Key Tuffite samples have a slightly more fractionated pattern than the andesite. These differences and any variation within the Key Tuffite itself, such as REE

fractionation, could be attributed to (1) physical processes, such as sorting (Fralick and Kronberg 1997) and fragmentation during a volcanic explosion (Wolff 1985; Horwell et al. 2001) and/or (2) chemical processes during explosion (Moune et al. 2006) or prolonged interaction between seawater and suspended ash particles (Sholkovitz et al. 1994). The Key Tuffite is only composed of fine ash resulting from an efficient process of subaqueous fragmentation. Thus, the Key Tuffite could have been highly susceptible to both the physical and chemical effects. Ultimately, hydrothermal alteration can also mobilize the LREE and Y (Finlow-Bates and Stumpfl 1981), which has been documented at Matagami in the Watson rhyolite footwall of several deposits (MacGeehan and MacLean 1980; MacLean 1988).

Our interpretation is that the Key Tuffite represents the explosive equivalent of the lower andesitic lava of the Wabassee and thus marks the initiation of the mafic volcanism. The volume of ash (up to10 m thick by >17 km in length north–south and by >1 km wide east–west) can be explained by a catastrophic explosive event or by a multitude of mafic eruption centres, as proposed by Sharpe (1968) based on the abundance of coarse breccias, and the lateral facies variations within the Wabassee. The lack of lateral variation in grain size, the well-developed planar beds and the uniform thickness of the Key Tuffite draping the topography of the Watson rhyolite indicate that the Key Tuffite formed as a waterlain tuff which saturated the water column (Gibson et al. 1999). The thin laminations preserved in the Key Tuffite suggest quiet depositional conditions in a relatively deep basin. The record of the progressive settling of the fine andesitic ash in suspension represents an important volcanic hiatus which was previously linked to the mineralization event (Liaghat and MacLean 1992; Maier et al. 1996). The intercalation of the Key Tuffite within the Watson rhyolite and the Dumagami rhyodacite or Bracemac rhyolite implies a synchronism/overlap between the beginning of the mafic lavas and the end of the felsic volcanic activity.

Exhalative component

Drill core observations at Bracemac-McLeod and underground observations at Perseverance (Figs. 8 and 9) provide evidence that the mineralization formed mainly by replacement processes. As a consequence, the exhalative component should be negligible in the Bracemac-McLeod and Perseverance vicinity and presumably elsewhere in the camp. This is commonly tested by a Fe/Ti versus Al/(Al + Mn + Fe) plot which is used to estimate the proportion of tuffaceous and exhalative components in ancient (Barrett 1981; Wonder et al. 1988; Peter et al. 2003) and modern (Boström 1973; Slack et al. 2009) deep-sea sediments. The Fe and Mn supposedly represent the exhalative contribution, whereas the Al and Ti represent the tuffaceous component. Liaghat and MacLean (1992) applied this plot for the Key Tuffite and the least altered volcanic rocks from Matagami. The entire set of Key Tuffite samples plot along a curve joining the clusters of fresh mafic and felsic rocks and the metalliferous sediments of the East Pacific Rise (Fig. 16a). Therefore, some samples were interpreted to be composed of more than 80 % of metalliferous sediments (Fig. 11 in Liaghat and MacLean 1992). However, altered Watson rhyolite and Wabassee andesite follow the same trend as the Key Tuffite (Fig. 16a) indicating that this trend does not only represent an exhalative contribution, but can also illustrate the alteration by an increase in sulfides (Fe) and chlorite (Fe + Mn) abundance. These results underline the limitations of this plot for deciphering the contribution of hydrothermal (exhalative or epigenetic) and tuffaceous component in an ancient and altered volcanic sequence.

Figure 16b represents a plot of Y/Ho versus Eu/Eu* (modified from Pinti et al. 2009) which has been proposed to discriminate chemical precipitation of chert versus replacement processes based on three endmembers: (1) high-temperature fluid (Douville et al. 1999); (2) Archean seawater, represented by Strelley Pool stromatolites (Van Kranendonk et al. 2003); and (3) andesite of the Wabassee Group, representing the tuffaceous component of the Key Tuffite. Silica precipitated from Archean seawater (Van Kranendonk et al. 2003) should have high Y/Ho ratios (~70) and moderately high europium anomalies (Eu/Eu*≈1). Exhalative chert should be a mixture of seawater and hydrothermal fluids (Pinti et al. 2009), the latter characterized by a positive europium anomaly (Eu/Eu*>>1). The replacement of tuff or volcanoclastic debris by silica from hydrothermal fluids would result in limited dispersion around the original composition of the precursor, which has low europium and Y anomalies. This graph shows that data from individual silicic layers analysed at Perseverance (Fig. 15) plot close to the Wabassee andesite and the Key Tuffite calculated precursor, indicating, in agreement with whole-rock Key Tuffite analyses, that replacement processes are dominant and that an exhalative component from high temperature fluids mixing with seawater is negligible around the Perseverance and Bracemac-McLeod deposits.

Epigenetic hydrothermal alteration component

Based on new high-precision U-Pb age of the Watson, Dumagami rhyodacite and Bracemac rhyolite, Ross et al. (2014) proposed that the Key Tuffite and mineralization were deposited on the seafloor between 2,725.9 and 2,725.4 Ma. However, field relationships between the mineralization and the Key Tuffite at Perseverance and Bracemac-McLeod (Fig. 8) and geochemistry of the Key Tuffite (Fig. 16) show that the mineralization was, for a major part, not coeval with the deposition of the Key Tuffite, but younger. Longuépée

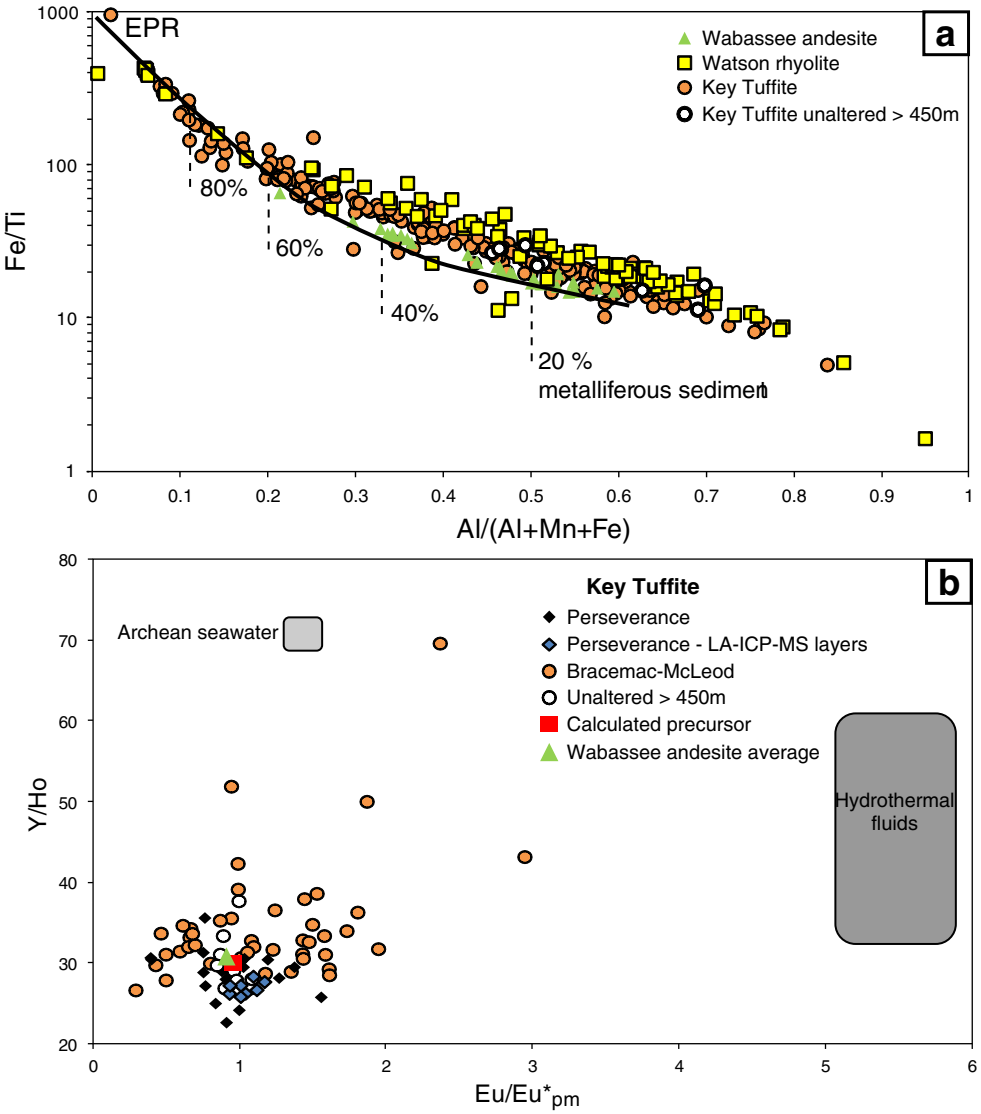

Fig. 16 Geochemical plots to determine any exhalative component in the Key Tuffite. **a** Fe/Ti versus Al/Al + Mn + Fe plot, modified from Boström (1973). Rhyolite and andesite data from Matagami (Glencore) for comparison. *EPR* East Pacific Rise metalliferous sediments. **b** Y/Ho versus Eu/Eu*pm plot, modified from Pinti et al. (2009). *pm* primitive mantle normalization from Sun and McDonough (1989)

(2009) documented that an alteration halo is present in the hanging wall of most of the deposits located along the south flank of Matagami. Although less extensive than that of the footwall, the alteration is similar in chemistry and persistent up to 40 m above the mineralization. This pattern, in agreement with our observations of mineralization within the Dumagami and Bracemac rhyolites, indicates that the main stage of mineralization occurred either during the deposition of the hanging wall rhyolites or that the VMS were mostly formed by sub-seafloor replacement. Consequently, the epigenetic alteration constitutes a significant component in the Key Tuffite, a feature confirmed by the mineral assemblage. The fine-grained mosaic of quartz, sericite, chlorite and carbonates is the typical hydrothermal alteration assemblage observed in the host rocks surrounding the mineralization at Matagami (Figs. 3, 4 and 7). The hydrothermally altered Key Tuffite laterally grades into unaltered equivalent rocks (Fig. 2). The lateral alteration of the Key Tuffite was geochemically tested using a mass gain and loss calculation versus the distance towards the deposits. The results (Fig. 14) show a coherent alteration pattern around the Bracemac-McLeod deposits: a proximal intense chloritization (<230 m) within a larger sericitization halo (230 to 400 m). Alteration halos present within the Watson rhyolite footwall are identical in chemistry and similar in dimension to the alteration halo in the Key Tuffite. It represents the first documentation of a coherent geochemical variation in the Key Tuffite toward a deposit in the Matagami mining camp and thus a useful vector for exploration.

Silicification and layering

Based on geochemistry, it is shown that the layering is not the product of mixing of two different sources of volcanic ash

(Fig. 10). The exhalative component is also negligible (Fig. 16), even in the finely layered chert zones (Fig. 15), confirming that layering is not the result of hydrothermal precipitation on the seafloor. Furthermore, layered and massive samples taken away from VMS deposits have a very similar composition indicating that the composition of the Key Tuffite is homogeneous at all scales (Figs. 11 and 15). As such, the thin planar layering is not the result of mixing multiple components, but instead the result of a progressive deposition of variable grain sizes of one type of ash in the water column (McPhie et al. 1993).

The apparent interbedding of silica, sulfide and chlorite in the Key Tuffite (Fig. 5) most likely resulted from selective replacement of more permeable ash layers, whereas the finer grained, and less permeable, layers remained less altered (Bodon and Valenta 1995; Galley et al. 1995; Doyle and Allen 2003). Layering is well developed only in the chert-rich sections of the Key Tuffite (Fig. 5b, f) suggesting that layering has been preserved and even highlighted by silicification. This process is well exposed at Perseverance where the silicification completely replaced the Key Tuffite in the vicinity of a synvolcanic fracture (Fig. 9a). This silicification overprints and destroys the primary bedding in the first 10–15 cm, on either side of the synvolcanic fracture, but is focussed laterally, for 30 cm or more, along three specific beds. Around it, the Key Tuffite is highly silicified, but the finer scale layering is preserved. A similar process of selective replacement of the primary layering is present in the Key Tuffite around Bracemac (Fig. 9b). The alteration halo around the synvolcanic fractures, which crosscuts the bedding at 45°, is very similar to the silica-rich layers. This indicates that hydrothermal fluids were laterally dispersed from the fractures when the porosity allowed it. However, some sub-parallel sulfide-rich veins crosscut the synvolcanic fractures, indicating that the mineralization of these specific layers occurred after the deposition of the Key Tuffite and after the silicification event. This is further evidence that the sulfide mineralization is not exhalative and overprints the complex hydrothermal history recorded by the Key Tuffite. Finally, another example from Orchan deposit area (Figs. 1 and 9c) confirms the selective alteration and replacement behaviour of the fluids along the most porous layers of the Key Tuffite. As for the Key Tuffite at Perseverance (Fig. 9a), the width of alteration halo surrounding the synvolcanic fracture is variable, probably as a function of the porosity of the layers infiltrated by the fluids.

Comparison with other mistaken exhalites

The term exhalite was introduced by Ridler (1971) and refers to the association of interbedded volcaniclastic (ash or sediments) and chemical precipitates (chert and sulfides) spatially related with VMS deposits. Such markers are useful indicators of the stratigraphic level of hydrothermal seafloor activity (Spry et al. 2000). In Archean VMS environments, these rocks are commonly interpreted as Algoma-type iron formations (Gross 1980; Spry et al. 2000). The classification of James (1954) distinguishes four predominant facies: sulfide, carbonate, oxide and silica. In various VMS contexts, strongly altered tuffaceous deposits comprising any one of these four facies have been mistaken for exhalites in the past. For example, the carbonate facies iron formation in the Hunter Mine Group (Superior Province, Quebec) is in fact the result of in situ low temperature replacement of chert and tuff beds (Chown et al. 2000). This hydrothermal activity is interpreted to be the result of late-stage volcanic activity and seawater infiltration. Similar processes have been documented in the Iberian Pyrite Belt (Leistel et al. 1997) where Fe-Mn carbonates and cherts were formed below the seafloor by replacement. The Helen Formation (Superior Province, Ontario) and the chlorite–tremolite–carbonate rocks associated with the Thalanga VMS (North Queensland, Australia), long considered as exhalative, also formed in a similar manner (Morton and Nebel 1984; Herrmann and Hill 2001). The omnipresence of silicification in VMS environments can also lead to erroneous interpretation of exhalite. For example, the ore-equivalent horizon of the Currawong Zn-Cu-Pb(-Au) massive sulfide deposit (Victoria, Australia) had been described as an exhalative unit until the selective replacement of sedimentary layers and the progressive gradation into fresh equivalent rocks were documented (Allen 1992; Bodon and Valenta 1995). Moreover, it was demonstrated that the inter-layering of sulfides within sedimentary rocks was the result of selective replacement of coarser layers. Our results imply that the Key Tuffite is another mistaken exhalite.

A replacement model for the formation of VMS at Matagami

The origin of the zinc-rich VMS deposits of the Matagami mining camp has long been debated. Previous studies showed evidence that the mineralization was in part epigenetic/replacement in several deposits along the south flank (e.g. Hallam 1964; Sharpe 1968; Clark 1983). Results of this study also imply that replacement is the dominant process over seafloor accumulation to form the Perseverance and Bracemac-McLeod deposits. The fluids are, however, synvolcanic in origin as demonstrated by the fluid inclusions (Ioannou et al. 2007). Thus, the link with the Key Tuffite is more spatial than genetic. The primary porous, water-saturated and glassy nature of the Key Tuffite makes it a favorable host for replacement-type mineralization or silicification as is common for unconsolidated volcanic debris layers (Doyle and Allen 2003).

Perseverance and Bracemac-McLeod not only represent the two extremities of the south flank, but also the two endmembers considering the geometry of the mineralized

lenses: discordant sub-vertical pods versus stratabound sheet-like. The general geometry of theses lenses is accepted to be mostly primary since the intensity of deformation along the south flank is weak (Piché et al. 1990; Lavallière et al. 1994) and incompatible with significant remobilization of ore. Despite their geometric differences, the formation of these two deposits is best explained by replacement processes. In both cases, ascending hydrothermal fluids were probably focused at depth by synvolcanic faults (Figs. 3 and 4). However, for Perseverance, the mineralization and hydrothermal alteration reflect the geometry of the sub-vertical structures themselves, indicating focused flow of hydrothermal fluids with minimal lateral dispersion into the volcanic succession. The overlying Key Tuffite is strongly altered (Fig. 11) but devoid of sulfides (Figs. 5f and 8b). The pervasive silicification in the Key Tuffite (Fig. 9a) and throughout the Dumagami rhyodacite hanging wall (Figs. 7a and 8a, b) could have occurred early in the life of the hydrothermal system by low-temperature fluids precipitating silica in pore spaces and fracture fillings. In this scenario, the Key Tuffite represents a cap rock sealing the roof of the system, being impermeable and refractory to mineralization. This process is common and important in replacive VMS processes (Jones et al. 2006; Schardt and Large 2009) as the mineralization is focalized beneath the impermeable alteration horizon (e.g. Gibson and Kerr 1993; Galley et al. 1995; Doucet et al. 1998; Sharpe and Gemmell 2001) and promotes thermal zone refining (Franklin 1995; Hannington et al. 1998). Similar geometry has been recognized in several VMS in Australia, where Mount Morgan and Reward (Large 1992) are good examples.

In contrast, at Bracemac-McLeod, the ascending fluids in synvolcanic structures were dispersed when they reached the porous Key Tuffite to produce widespread stratabound alteration (Fig. 14). The sheet-style massive sulfide orebodies of Bracemac-McLeod suggest a progressive replacement induced by fluid percolation focused along the Key Tuffite but also replacing the hyaloclastic upper part of the Watson Group (Fig. 8d). This last process was documented for the Mattagami Lake mine where the top of the Watson rhyolite is described as thick vitroclastic mineralized tuff (Roberts 1975; Roberts and Reardon 1978), hence highlighting the importance of the volcanic permeability for replacement. Similar sheet-like and low aspect ratio deposits have been described in Australia and are commonly considered to be formed by synvolcanic subseafloor replacement. The best examples are Rosebery, Thalanga and Scuddles (Large 1992; Allen 1994).

Replacement processes have probably been underestimated in previous studies of the VMS deposits in the Matagami mining camp due to the obvious link with the Key Tuffite. Indeed, the exhalative model is not the most efficient mineralization process since it has been estimated that 99 % of the metals from hydrothermal vents are dispersed in the ocean (Rona 1984). The replacement model better accounts for the very high zinc grade of the Matagami VMS deposits.

For exploration, the Key Tuffite represents a major volcanic hiatus and the transition from felsic- to mafic-dominated volcanism. The hydrothermal activity probably started during the deposition of the Key Tuffite and could have contributed to form some VMS deposits as suggested previously (e.g. Lavallière et al. 1994). However, Perseverance and Bracemac-McLeod highlight the fact that the hydrothermal activity continued after the deposition of a part of the Wabassee Group (after 2,725.8 Ma, Ross et al. 2014). The mineralization was controlled by the porosity of the overlying volcanic facies (Key Tuffite and hyaloclastic top of the Watson rhyolite) and synvolcanic structures suggesting that economic mineralization could be found at other stratigraphic levels if the permeability allowed mineralizing fluid flow. However, the Key Tuffite is important because in most cases, it was the first thick porous unit that the mineralizing fluids encountered during their migration towards the seafloor.

Conclusions

The Key Tuffite is spatially linked with all the exploited zinc-rich VMS deposits in the Matagami mining camp. Previously thought to be exhalative in origin, new field observations and geochemical data at the Perseverance and Bracemac-McLeod deposits demonstrate that the exhalative component is negligible or absent. The unit is only composed of andesitic ash, which probably represents the explosive equivalent of the first mafic units of the overlying Wabassee Group. The mineralization event was dominantly epigenetic and occurred most likely as sub-seafloor replacement. Mineralizing fluids used synvolcanic structures and replaced units such as the Key Tuffite or the hyaloclastic top of the Watson rhyolite. A coherent geochemical alteration pattern in the Key Tuffite can be used as a vector towards VMS mineralization in the Matagami Camp. The VMS mineralization is not limited to the Key Tuffite level and is partly controlled by the permeability of the volcanic facies.

Acknowledgments This Ph.D. project is a part of a larger research program on the Matagami mining camp, including a volcanology Ph.D. (INRS-Quebec) and a geophysical Ph.D. (École Polytechnique-Montreal). Financial support for this study was provided by NSERC, CONSOREM, DIVEX, Geological Survey of Canada, Glencore (Previously Xstrata Zinc), Donner Metals, SOQUEM and Nyrstar (previously Breakwater Resources). We thank the companies for the authorization to diffuse these results. J-A Debreil and R. Daigneault are thanked for useful discussions. R. Adair (Donner Metals) is additionally thanked for his informal review of a preliminary version of the document. N. Yapi is thanked for collecting samples in 2008. A. Paulin-Bissonnette is also thanked for his contribution as undergraduate field assistant during the

summer 2010. We are grateful to S.A.S. Dare, Research Associate at UQAC, for proofreading the English text. Finally, the manuscript greatly benefited from comments and suggestions by D. Lentz and P. Mercier-Langevin. Thanks are given to T. Bissig and G. Beaudoin for their editorial handling.

References

Adair R (2009) Technical report on the resource calculation for the Bracemac-McLeod discoveries, Matagami Project, Québec. Donner Metals Ltd., National Instrument 43-101 Report, Vancouver, Canada, pp 194. http://www.sedar.com. Accessed 3 Apr 2009

Allen RL (1992) Reconstruction of the tectonic, volcanic, and sedimentary setting of strongly deformed Zn-Cu massive sulfide deposits at Benambra, Victoria. Econ Geol 87:825–854

Allen RL (1994) Syn-volcanic, subseafloor replacement model for Rosebery and other massive sulfide ores [abs.]. Contentious issues in Tasmanian Geology Symposium. Geological Society of Australia Tasmanian Division 89-91

Allen RL, Weihed P (2002) Global comparisons of volcanic-associated massive sulphide districts. Geol Soc Lond Spec Publ 204:13–37

Arnold G (2006) Perseverance deposit geology: Falconbridge Limited (now Glencore). Internal report 101

Baldwin GJ, Thurston PC, Kamber BS (2011) High-precision rare earth element, nickel, and chromium chemistry of chert microbands pre-screened with in-situ analysis. Chem Geol 285:133–143

Barrett TJ (1981) Chemistry and mineralogy of Jurassic bedded chert overlying ophiolites in the North Apennines, Italy. Chem Geol 34: 289–317

Barrett TJ, MacLean WH (1999) Volcanic sequences, lithogeochemistry, and hydrothermal alteration in some bimodal volcanic-associated massive sulfide systems. In: Barrie CT, Hannington MD (eds) Reviews in economic geology, vol. 8. Society of Economic Geologists, pp. 101–131

Barrett TJ, MacLean WH, Årebäck H (2005) The Palaeoproterozoic Kristineberg VMS deposit, Skellefte district, northern Sweden. Part II: chemostratigraphy and alteration. Miner Deposita 40:368–395

Beaudry C, Gaucher E (1986) Cartographie géologique dans la région de Matagami: Québec. Ministère de l'énergie et des Ressources, Rapport MB 86-32, pp 147

Bierlein FP (1995) Rare-earth element geochemistry of clastic and chemical metasedimentary rocks associated with hydrothermal sulphide mineralisation in the Olary Block, South Australia. Chem Geol 122: 77–98

Bloom L, Beaudry C (2009) Evidence of 25-m of vertical metal migration over the high-grade Perseverance zinc ore body, Matagami, Quebec. Proceedings of the 24th IAGS. Fredericton, pp 357-359

Bodon SB, Valenta RK (1995) Primary and tectonic features of the Currawong Zn-Cu-Pb(-Au) massive sulfide deposit, Benambra, Victoria; implications for ore genesis. Econ Geol 90:1694–1721

Boström K (1973) The origin of ferromanganoan active ridge sediments. Stockh Contrib Geol 27:149–243

Bussières Y, Théberge D (2006) Rapport technique NI 43-101, concernant la propriété Caber–Du Dôme, Secteur de Matagami, Nord-ouest du Québec, région de l'Abitibi. pp 125

Card KD (1990) A review of the Superior Province of the Canadian Shield, a product of Archean accretion. Precambrian Res 48:99–156

Carr PM, Cathles LM, Barrie CT (2008) On the size and spacing of volcanogenic massive sulfide deposits within a district with application to the Matagami District, Quebec. Econ Geol 103: 1395–1409

Chown EH, N'dah E, Mueller WU (2000) The relation between iron-formation and low temperature hydrothermal alteration in an Archean volcanic environment. Precambrian Res 101:263–275

Clark JR (1983) The geology and trace element distributions of the sulfide bodies at Orchan mine, Matagami. Colorado School of Mines, Quebec

Corliss JB, Dymond J, Gordon LI, Edmond JM, von Herzen RP, Ballard RD, Green K, Williams D, Bainbridge A, Crane K (1979) Submarine thermal springs on the Galapagos Rift. Science 203:1073–1083

Costa UR, Barnett RL, Kerrich R (1983) The Mattagami Lake Mine Archean Zn-Cu sulfide deposit, Quebec; hydrothermal coprecipitation of talc and sulfides in a sea-floor brine pool; evidence from geochemistry, 18 O/16 O, and mineral chemistry. Econ Geol 78:1144–1203

Côté A, Lavigne M (2010) Report and feasibility study for the Bracemac-McLeod Project Matagami Area Quebec. (Xstrata Zinc and Genivar Limited Partnership), pp 315

Daigneault R, Mueller WU, Chown EH (2004) Abitibi greenstone belt plate tectonics: the diachronous history of arc development, accretion and collision. In: Eriksson PG, Altermann W, Nelson DR, Mueller WU, Catuneau O, Strand K (eds) Developments in Precambrian geology/tempos of events in Precambrian time. Elsevier, Amsterdam, pp 88–103

Davidson AJ (1977) Petrography and chemistry of the Key Tuffite at Bell Allard. McGill University, Matagami, Quebec, p 131

Debreil J, Ross P-S (2009) Volcanic architecture of the Matagami Mining Camp: implications for mineral exploration. AGU Spring Meeting Abstracts #V31B-17. pp 17

Doucet P, Mueller W, Chartrand F (1998) Alteration and ore mineral characteristics of the Archean Coniagas massive sulfide deposit, Abitibi belt, Quebec. Can J Earth Sci 35:620–636

Douville E, Bienvenu P, Charlou JL, Donval JP, Fouquet Y, Appriou P, Gamo T (1999) Yttrium and rare earth elements in fluids from various deep-sea hydrothermal systems. Geochim Cosmochim Acta 63:627–643

Doyle MG, Allen RL (2003) Subsea-floor replacement in volcanic-hosted massive sulfide deposits. Ore Geol Rev 23:183–222

Eastoe CJ, Solomon M, Walshe JL (1987) District-scale alteration associated with massive sulfide deposits in the Mount Read Volcanics, western Tasmania. Econ Geol 82:1239–1258

Finlow-Bates T, Stumpfl EF (1981) The behaviour of so-called immobile elements in hydrothermally altered rocks associated with volcanogenic submarine-exhalative ore deposits. Mineral Deposita 16:319–328

Fralick PW, Kronberg BI (1997) Geochemical discrimination of clastic sedimentary rock sources. Sediment Geol 113:111–124

Franklin JM (1995) Volcanic-associated massive sulphide base metals. Geol Can 8:158–183, Geological Survey of Canada

Franklin JM, Sangster DF, Lydon JW (1981) Volcanic-associated massive sulfide deposits. Economic Geology 75th Anniversary Volume: 485-627

Gaboury D, Pearson V (2008) Rhyolite geochemical signatures and association with volcanogenic massive sulfide deposits: examples from the Abitibi Belt, Canada. Econ Geol 103:1531–1562

Galley AG (1993) Characteristics of semi-conformable alteration zones associated with volcanogenic massive sulphide districts. J Geochem Explor 48:175–200

Galley AG, Watkinson DH, Jonasson IR, Riverin G (1995) The subsea-floor formation of volcanic-hosted massive sulfide; evidence from the Ansil Deposit, Rouyn-Noranda, Canada. Econ Geol 90:2006–2017

Gemmell JB, Fulton R (2001) Geology, Genesis, and exploration implications of the footwall and hanging-wall alteration associated with the Hellyer volcanic-hosted massive sulfide deposit, Tasmania, Australia. Econ Geol 96:1003–1035

Gibson HL, Kerr DJ (1993) Giant volcanic-associated massive sulphide deposits: with emphasis on Archean examples. Econ Geol Spec Publ 2:319–348

Gibson HL, Morton RL, Hudak GJ (1999) Submarine volcanic processes, deposits and environments favorable for the location of volcanic-associated massive sulfide deposits. Rev Econ Geol 8:13–51

Gross GA (1980) A classification of iron formations based on depositional environments. Can Mineral 18:215–222

Hallam R (1964) Matagami Lake Mines Ltd., some aspects of the geology and ore control. Bull Can Inst Min Metall 57:389–396

Hannington MD, Galley AG, Herzig PM, Petersen S (1998) Comparison of the TAG mound and stockwork complex with Cyprus-type massive sulfide deposits. Proc Ocean Drill Program Sci Results 158: 389–415

Hart TR, Gibson HL, Lesher CM (2004) Trace element geochemistry and petrogenesis of felsic volcanic rocks associated with volcanic massive Cu-Zn-Pb sulfide deposits. Econ Geol 99:1003–1013

Herrmann W, Hill AP (2001) The origin of chlorite-tremolite-carbonate rocks associated with the Thalanga volcanic-hosted massive sulfide deposit, North Queensland, Australia. Econ Geol 96:1149–1173

Horwell CJ, Braña LP, Sparks RSJ, Murphy MD, Hards VL (2001) A geochemical investigation of fragmentation and physical fractionation in pyroclastic flows from the Soufrière Hills volcano, Montserrat. J Volcanol Geotherm Res 109:247–262

Ioannou SE, Spooner ETC (2007) Fracture analysis of a volcanogenic massive sulfide-related hydrothermal cracking zone, Upper Bell River Complex, Matagami, Quebec: application of permeability tensor theory. Econ Geol 102:667–690

Ioannou SE, Spooner ETC, Barrie CT (2007) Fluid temperature and salinity characteristics of the Matagami volcanogenic massive sulfide district, Quebec. Econ Geol 102:691–715

James HL (1954) Sedimentary facies of iron-formation. Econ Geol 49: 235–293

Jenney CP (1961) Geology and ore deposits of the Mattagami area, Quebec. Econ Geol 56:740–757

Jolly WT (1978) Metamorphic history of the Archean Abitibi belt. In: Fraser JA, Heywood WW (eds) Metamorphism in the Canadian Shield. Geological Survey of Canada, Paper 78-10, pp 63-78

Jones S, Gemmell JB, Davidson GJ (2006) Petrographic, geochemical, and fluid inclusion evidence for the origin of siliceous cap rocks above volcanic-hosted massive sulfide deposits at Myra Falls, Vancouver Island, British Columbia, Canada. Econ Geol 101:555–584

Kalogeropoulos SI, Scott SD (1983) Mineralogy and geochemistry of tuffaceous exhalites (tetsusekiei) of the Fukazawa mine, Hokuroku district, Japan. Econ Geol Monogr 5:412–432

Large RR (1992) Australian volcanic-hosted massive sulfide deposits; features, styles, and genetic models. Econ Geol 87:471–510

Large RR, Allen RL, Blake MD, Herrmann W (2001a) Hydrothermal alteration and volatile element halos for the Rosebery K Lens volcanic-hosted massive sulfide deposit, Western Tasmania. Econ Geol 96:1055–1072

Large RR, Gemmell JB, Paulick H, Huston DL (2001b) The alteration box plot: a simple approach to understanding the relationship between alteration mineralogy and lithogeochemistry associated with volcanic-hosted massive sulfide deposits. Econ Geol 96:957–971

Latulippe M (1959) Mattagami area of northwestern Quebec. Geol Assoc Can Proc 2:45–54

Lavallière G, Guha J, Daigneault R (1994) Cheminées de sulfures massifs atypiques du gisement d'Isle-Dieu, Matagami, Québec; implications pour l'exploration. Explor Min Geol 3:109–129

Leistel JM, Marcoux E, Deschamps Y (1997) Chert in the Iberian pyrite belt. Miner Deposita 33:59–81

Lesher CM, Goodwin AM, Campbell IH, Gorton MP (1986) Trace-element geochemistry of ore-associated and barren, felsic metavolcanic rocks in the Superior Province, Canada. Can J Earth Sci 23:222–237

Liaghat S, MacLean WH (1992) The Key Tuffite, Matagami mining district; origin of the tuff components and mass changes. Explor Min Geol 1:197–207

Longuépée H (2009) Empreinte hydrothermale au toit de sulfures massifs volcanogènes. Rapport du projet CONSOREM 2007-05. pp 33

Lydon JW (1988) Volcanogenic massive sulphide deposits part 2: genetic models. Geosci Can Reprints Ser 3:155–182

MacGeehan PJ, MacLean WH (1980) An Archaean sub-seafloor geothermal system, 'calc-alkali' trends, and massive sulphide genesis. Nature 286:767–771

MacLean WH (1988) Rare earth element mobility at constant inter-REE ratios in the alteration zone at the Phelps Dodge massive sulphide deposit, Matagami, Quebec. Miner Deposita 23:231–238

MacLean WH, Davidson AJ (1977) Case history of the Bell-Allard Mine, Matagami, Quebec. Mineral Exploration Research Institute, Paper 77-3, pp 55

MacLean WH, Kranidiotis P (1987) Immobile elements as monitors of mass transfer in hydrothermal alteration; Phelps Dodge massive sulfide deposit, Matagami, Quebec. Econ Geol 82:951–962

Maier WD, Barnes S-J, Pellet T (1996) The economic significance of the Bell River Complex, Abitibi subprovince, Quebec. Can J Earth Sci 33:967–980

Masson M (2000) Option Caber, rapport de sondages 1998-1999. Noranda Inc, Travaux statutaires déposés au Ministère des Ressources naturelles (Québec), GM 58074. pp 36

McPhie J, Doyle M, Allen R (1993) Volcanic textures: a guide to the interpretation of textures in volcanic rocks. CODES Key Centre. University of Tasmania, Hobart, p 196

Mercier-Langevin P, Goutier J, Ross P-S, McNicoll VJ, Monecke T, Dion C, Dubé B, Thurston P, Bécu V, Gibson HL, Hannington MD, Galley AG (2011) The Blake River Group of the Abitibi greenstone belt and its unique VMS and gold-rich VMS endowment GAC-MAC-SEG-SGA Joint Annual Meeting 2011, Ottawa, Field Trip 02B guidebook; Geological Survey of Canada, Open File report 6869. pp 61.

Mercier-Langevin P, Gibson HL, Hannington MD, Goutier J, Monecke T, Dubé B, Houlé MG (2014) A special issue on Archean magmatism, volcanism, and ore deposits: part 2. Volcanogenic massive sulfide deposits preface. Econ Geol 109:1–9

Miller RJM (1960) Geology of Mattagami Lake mines. Can Inst Min Metall Bull 53:194

Mortensen JK (1993) U–Pb geochronology of the eastern Abitibi Subprovince. Part 1: Chibougamau–Matagami–Joutel region. Can J Earth Sci 30:11–28

Morton RL, Nebel ML (1984) Hydrothermal alteration of felsic volcanic rocks at the Helen siderite deposit, Wawa, Ontario. Econ Geol 79:1319–1333

Moune S, Gauthier P-J, Gislason SR, Sigmarsson O (2006) Trace element degassing and enrichment in the eruptive plume of the 2000 eruption of Hekla volcano, Iceland. Geochim Cosmochim Acta 70:461–479

Mueller WU, Daigneault R, Mortensen JK, Chown EH (1996) Archean terrane docking: upper crust collision tectonics, Abitibi greenstone belt, Quebec, Canada. Tectonophysics 265:127–150

Mueller WU, Stix J, Corcoran PL, Daigneault R (2009) Subaqueous calderas in the Archean Abitibi greenstone belt: an overview and new ideas. Ore Geol Rev 35:4–46

Munoz Taborda CM (2011) Distribution of platinum-group elements in the Ebay claim, central part of the Bell River Complex, Matagami, Quebec. Université du Québec à Chicoutimi, pp 206

Ohmoto H (1996) Formation of volcanogenic massive sulfide deposits: the Kuroko perspective. Ore Geol Rev 10:135–177

Peter JM, Goodfellow WD (2003) Hydrothermal sedimentary rocks of the Heath Steele belt, Bathurst mining camp, New Brunswick: part 3. Application of mineralogy and mineral and bulk compositions to massive sulfide exploration. Econ Geol Monogr 11:417–433

Peter JM, Goodfellow WD, Doherty W (2003) Hydrothermal sedimentary rocks of the Heath Steele Belt, Bathurst mining camp, New

Brunswick: part 2. Bulk and rare earth element geochemistry and implications for origin. Econ Geol Monogr 11:391–415

Piché M, Guha J, Daigneault R, Sullivan JR, Bouchard G (1990) Les gisements volcanogènes du camp minier de Matagami: structure, stratigraphie et implications métallogéniques. Can Inst Min Met Spec Vol 43:327–336

Piché M (1991) Synthèse géologique et métallogénique du camp minier de Matagami, Québec. Université du Québec à Chicoutimi, pp 269

Piché M, Guha J, Daigneault R (1993) Stratigraphic and structural aspects of the volcanic rocks of the Matagami mining camp, Quebec; implications for the Norita ore deposit. Econ Geol 88:1542–1558

Pilote P, Debreil J-A, Williamson K, Rabeau O, Lacoste P (2011) Révision géologique de la région de Matagami. Québec exploration—Poster 276. Québec

Pinti DL, Hashizume K, Sugihara A, Massault M, Philippot P (2009) Isotopic fractionation of nitrogen and carbon in Paleoarchean cherts from Pilbara craton, Western Australia: origin of 15N-depleted nitrogen. Geochim Cosmochim Acta 73:3819–3848

Ridler RH (1971) Analysis of Archean volcanic basins in the Canadian shield using the exhalite concept [abs.]. Bull Can Inst Min Metall 64: 20

Roberts RG (1975) The geological setting of the Mattagami Lake Mine, Quebec: a volcanogenic massive sulfide deposit. Econ Geol 70:115–129

Roberts RG, Reardon EJ (1978) Alteration and ore-forming processes at Mattagami Lake Mine, Quebec. Can J Earth Sci 15:1–21

Rona PA (1984) Hydrothermal mineralization at seafloor spreading centers. Earth Sci Rev 20:1–104

Ross P-S, McNicoll VJ, Debreil JA, Carr PM (2014) Precise U-Pb geochronology of the Matagami mining camp, Abitibi Greenstone Belt, Quebec: stratigraphic constraints and implications for volcanogenic massive sulfide exploration. Econ Geol 109:89–101

Sangster D (1972) Precambrian volcanogenic massive sulphide deposits in Canada: a review. Geol Surv Can Pap 72–22:44

Schardt C, Large RR (2009) New insights into the genesis of volcanic-hosted massive sulfide deposits on the seafloor from numerical modeling studies. Ore Geol Rev 35:333–351

Sharpe JI (1968) Géologie et gisements de sulfures de la région de Matagami, Comté d'Abitibi-Est, Québec. Ministère des Richesses Naturelles du Québec. Rapp Géol 137:122

Sharpe R, Gemmell JB (2001) Alteration characteristics of the Archean Golden Grove Formation at the Gossan Hill Deposit, Western Australia: induration as a focusing mechanism for mineralizing hydrothermal fluids. Econ Geol 96:1239–1262

Sholkovitz ER, Landing WM, Lewis BL (1994) Ocean particle chemistry: the fractionation of rare earth elements between suspended particles and seawater. Geochim Cosmochim Acta 58:1567–1579

Slack JF, Grenne T, Bekker A (2009) Seafloor-hydrothermal Si-Fe-Mn exhalites in the Pecos greenstone belt, New Mexico, and the redox state of ca. 1720 Ma deep seawater. Geosphere 5:302–314

Spry PG, Peter JM, Slack JF (2000) Meta-exhalites as exploration guides to ore. Rev Econ Geol 11:163–201

Sun S-S, McDonough WF (1989) Chemical and isotopic systematics of oceanic basalts: implications for mantle composition and processes. Geol Soc Lond Spec Publ 42:313–345

Tully DW (1964) Notes on the geology of the no. 1 orebody, Mattagami Lake Mines Ltd. Can Inst Min and Met Field Excursion Guide Book: 7–19

Van Kranendonk MJ, Webb GE, Kamber BS (2003) Geological and trace element evidence for a marine sedimentary environment of deposition and biogenicity of 3.45 Ga stromatolitic carbonates in the Pilbara Craton, and support for a reducing Archaean ocean. Geobiology 1:91–108

Winchester JA, Floyd PA (1977) Geochemical discrimination of different magma series and their differentiation products using immobile elements. Chem Geol 20:325–343

Wolff JA (1985) The effect of explosive eruption processes on geochemical patterns within pyroclastic deposits. J Volcanol Geotherm Res 26:189–201

Wonder JD, Spry PG, Windom KE (1988) Geochemistry and origin of manganese-rich rocks related to iron-formation and sulfide deposits, western Georgia. Econ Geol 83:1070–1081